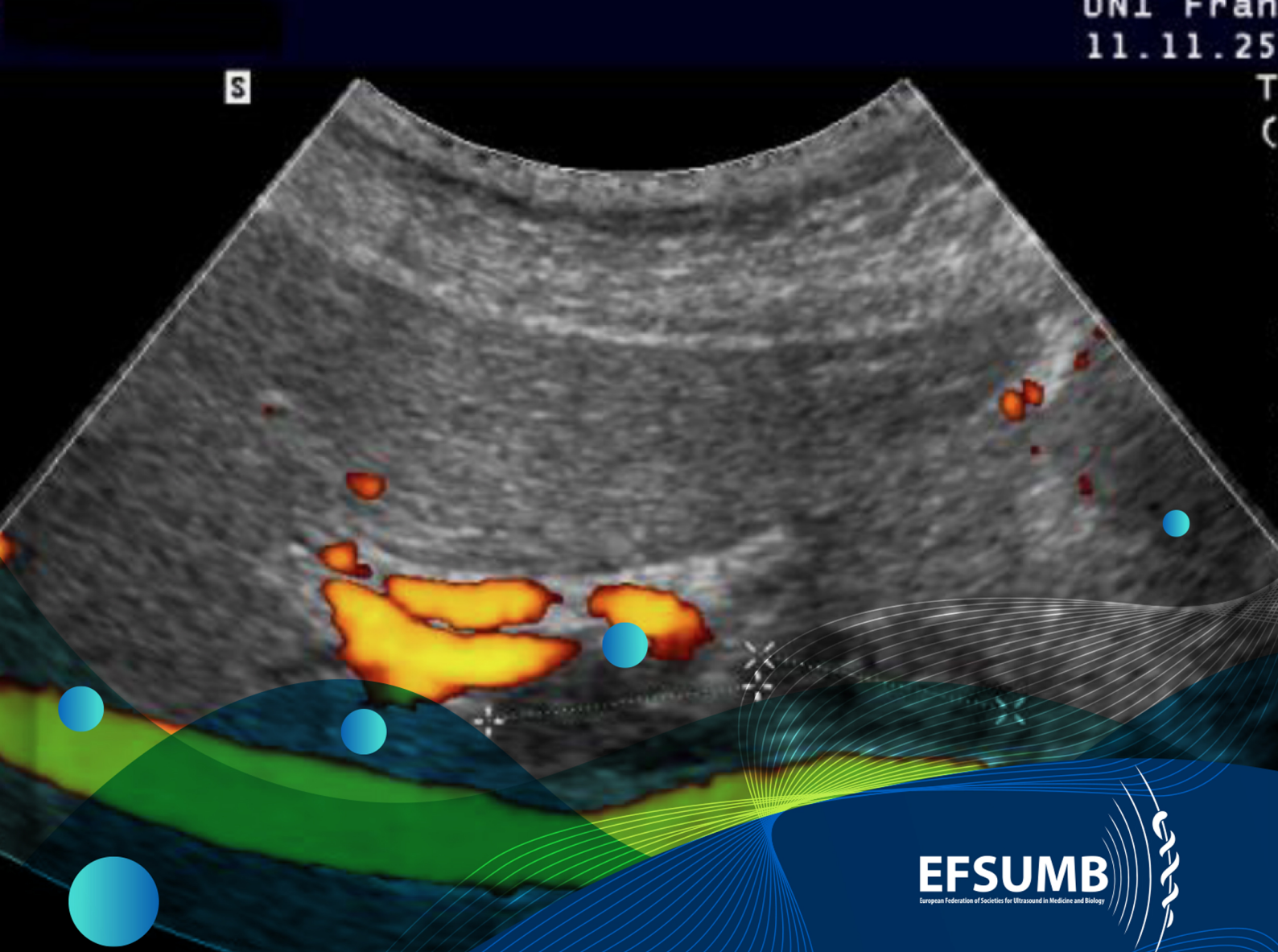

EFSUMB
European Federation of Societies for Ultrasound in Medicine and Biology

EFSUMB Course Book

2nd Edition

Editor: Christoph F. Dietrich

Ch 22: Human immunodeficiency virus (HIV) infection and tuberculosis (TB)

Tom Heller[2], Michaela AM Huson[2], Maria-Theresa Giordano[3], Enrico Brunetti[4], Christoph F Dietrich[5]

1. Lighthouse Clinic Trust, Lilongwe, Malawi.
2. Section of Infectious Diseases, Department of Internal Medicine, Erasmus MC University Medical Centre Rotterdam, Rotterdam, Netherlands.
3. Department of Infectious Diseases, San Bortolo Hospital, Vicenza, Italy.
4. Infectious and Tropical Diseases. IRCCS San Matteo Hospital Foundation-University of Pavia. WHO Collaborating Centre for Clinical Management of Cystic Echinococcosis. Pavia, Italy.
5. Department Allgemeine Innere Medizin in Hirslanden Kliniken Beau Site, Salem and Permanence in Berne, Switzerland

Corresponding author: Prof. Dr. Christoph F. Dietrich, MBA. Medizinische Klinik 2, Caritas-Krankenhaus Bad Mergentheim, Uhlandstr. 7, 97980 Bad Mergentheim. Tel.: (+) 49 - 7931 – 58 – 2201. Fax: (+) 49 - 7931 – 58 – 2290. Email: christoph.dietrich@ckbm.de

Acknowledgments: The authors thank Rosie Conlon, Carlo Filice and Sam Goblirsch for their work on the previous version of this chapter. The authors also thank Hein Lamprecht for review.

Introduction

Human immunodeficiency virus (HIV) infection and tuberculosis (TB) are two diseases that are frequently seen together. The twin epidemics especially affect Sub-Saharan Africa, but they are synergistic in other areas of the world as well [(1)]. Besides socio–economic causes, there are biological explanations for this concurrence. With HIV disease progression, the probability of reactivation of latent TB infection increases; the incidence of active TB has been found to be increase more than twentyfold in those who are HIV-positive compared with HIV-negative individuals [(2, 3)]. Furthermore, HIV infection increases the risk of progression to active TB after primary infection [(4)]. At the same time, active TB favours early viral replication and dissemination and therefore contributes to the progression of HIV-1 infection [(5)]. As both diseases frequently affect patients simultaneously, their ultrasound findings will be covered together in this chapter.

Human Immunodeficiency Virus (HIV)

Introduction

HIV is a chronic infection mainly affecting the T-helper cells ('CD4 cells'). In untreated infections, destruction of CD4 T-helper lymphocytes leads to an increasing degree of immune suppression, especially when the CD4 count falls below 350 cells/mm^3. While infections with HIV have become a manageable chronic condition in Europe where effective antiretroviral treatment (ART) has made severe immunosuppression a rarity, it is still a major cause of morbidity and mortality in tropical countries, especially in sub-Saharan Africa. The programmatic roll-out of ART is successfully advancing and the Global Burden of Disease Study, published in in October 2016 [(6)], showed a significant increase in life expectancy between 2005 and 2015 in many African countries (e.g. patients in Malawi gained life expectancy of 13.7 years for females and 10.5 years for males) mainly due to ART. Recent changes in the WHO guidelines have seen a move towards people starting ART at higher CD4 counts and since 2016 the recommendation has been to treat all HIV positive patients in all settings irrespective of their CD4 count [(7)]. The *test-and-treat strategy* carries the optimism that 'sick patients' can be prevented. Despite the guideline changes a substantial proportion

of people do not get diagnosed or initiated on ART until their CD4 counts are very low, which prompted further WHO guidelines on the management of these 'advanced patients' [(8)]. When CD4 counts fall below 200 cells/mm^3, a variety of opportunistic infections and malignancies affect the patient who is then diagnosed with acquired immunodeficiency syndrome (AIDS) [(9)].

Ultrasound is useful in the diagnosis of a wide array of HIV associated diseases and infections in various organ systems, predominantly in diagnosing opportunistic infections in severely immunosuppressed patients, but also in patients with longstanding HIV infection on ART [(10, 11)]. In addition, it is widely used to guide diagnostic needle biopsies for histological or microbiological investigations [(12)]. The use of point-of-care ultrasound is being recorded in an increasing number of regions [(13, 14)]. This section is an overview of ultrasound findings that may be seen in the organs of patients with HIV.

Abdominal ultrasound

Liver

Diffuse pathologies

Hepatomegaly is one of the most frequent findings in patients who are HIV-positive and was found in up to 35% of patients screened in the Democratic Republic of Congo and Zambia [(15, 16)]. The causes of hepatomegaly in HIV-positive patients are numerous, but the most frequent are concomitant hepatitis B and C virus infection, cytomegalovirus (CMV) infection, granulomatous hepatitis *e.g.* due to tuberculosis [(17)], *Mycobacterium tuberculosis*, atypical mycobacteria infection (MOTT, mycobacteria other than tuberculosis, e.g. mycobacterium avium complex (MAC) or *Mycobacterium kansasii*) and diffuse lymphomatous infiltration [(18, 19)]. Visceral leishmaniasis, presenting with fever and hepatosplenomegaly, is also more common in people infected with HIV and is an important differential in endemic areas [(20)]. In Asia, *Talaromyces* (formerly *Penicillium*) *marneffei* is a common opportunistic infection causing hepatosplenomegaly and generalised lymphadenopathy, as well as typical skin lesions [Figure 1].

Figure 1 **Diffuse hepatomegaly (a) and splenomegaly (b) (17 cm) in a patient with *Talaromyces marneffei* infection. Typical umbilicated skin lesion on the forearm (c).**

a

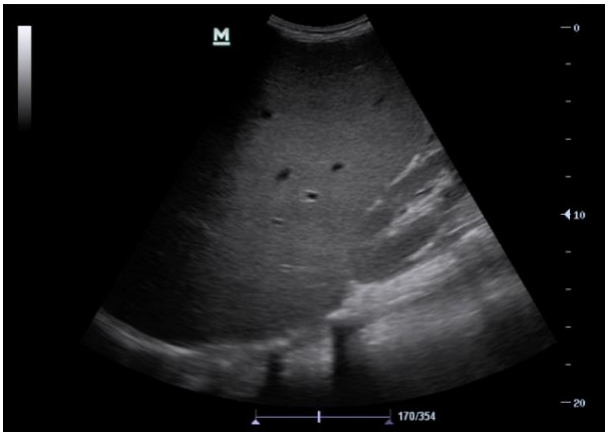

b

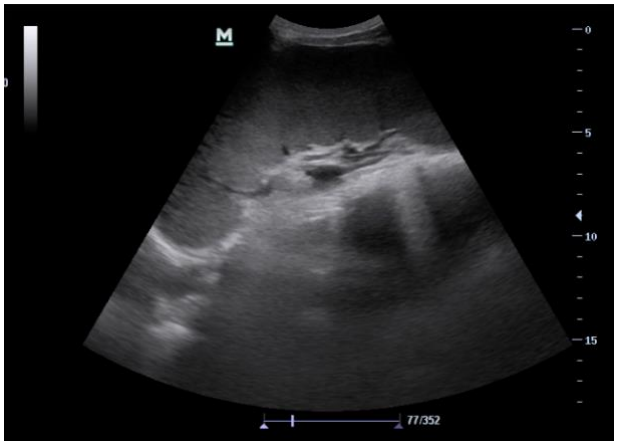

c

Often no specific cause of hepatomegaly is found. Ultrasound-guided liver biopsy helps to narrow down the differential diagnosis. Small lymph nodes are frequently detectable within the hepatoduodenal ligament in patients with chronic HIV. Enlarged lymph nodes can be found in HIV-positive patients with or without chronic hepatitis C virus [(21-23)] and in other inflammatory liver diseases such as primary biliary cholangitis and autoimmune hepatitis [(19, 24-26)], as well as in lymphoma [Figure 2].

Figure 2 Enlarged perihepatic lymph nodes in the dorsal hepatoduodenal ligament (between markers) in an HIV-positive patient with chronic hepatitis C and hepatic tuberculosis.

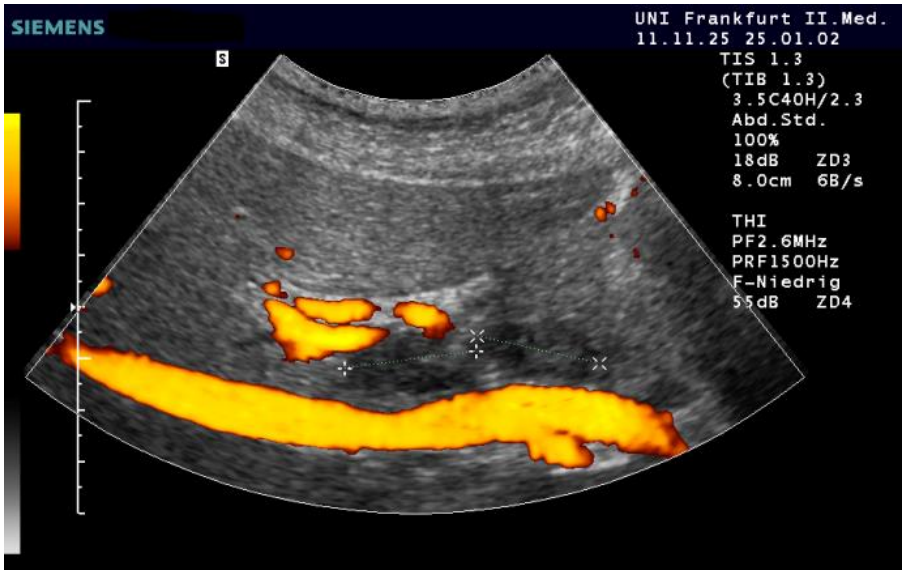

Focal pathologies

Focal pathologies of the liver are a common finding in patients with HIV. The echo-pattern of the liver lesions may be described as hypoechoic, hyperechoic or of mixed echogenicity. Diseases commonly presenting with hypoechoic liver lesions are lymphoma, *Mycobacterium tuberculosis* infection and abscesses [(27)]. AIDS-related lymphomatous lesions may vary largely in size from a few to several centimetres [Figure 3] and in some instances they may appear echo-free and can be confused with cystic lesions [Figure 4]. Bacterial abscesses often show irregular borders and may contain small gas bubbles [Figure 5].

Figure 3 Complex lesion in the left lobe of the liver in a patient with HIV: lymphoma.

Figure 4 Round hypoechoic lesion in the liver of an HIV positive patient: non-Hodgkin lymphoma (biopsy result).

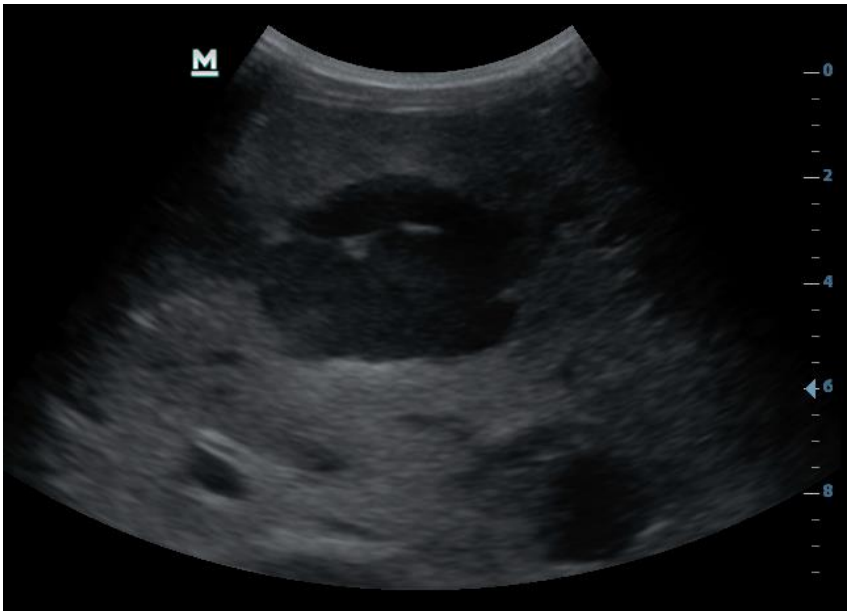

Figure 5 Bacterial abscess of the liver.

Fungal microabscesses can have a bulls-eye appearance; in particular, this morphology has been described in *Candida albicans* infections and mucormycosis [(11)] [Figure 6].

Disseminated Kaposi's sarcoma (KS) presents with hyperechoic, disseminated lesions, 5–10 mm in size, which can be found even in the absence of cutaneous lesions [Figure 7]. In larger KS lesions, a complex echo-pattern with hyper- and hypoechoic areas is observed.

Figure 6 'Bull's eye' sonographic appearance of a fungal abscess in the liver of an HIV-positive young drug user [(11)].

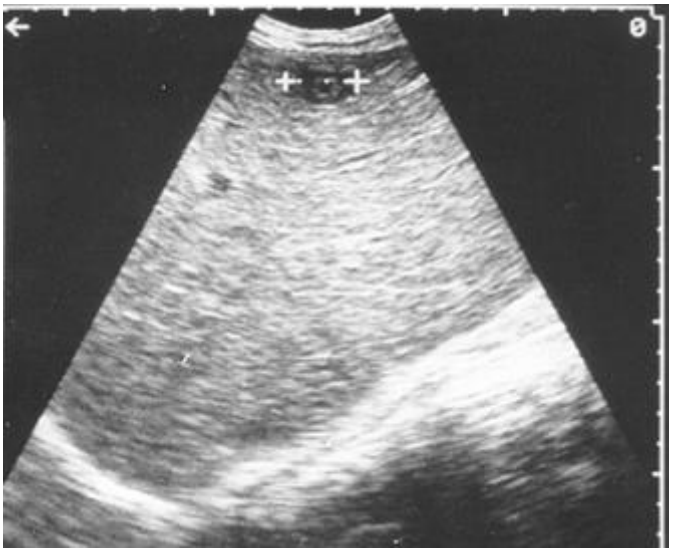

Figure 7 Hyperechoic liver lesion in an HIV positive patient with disseminated Kaposi's sarcoma: liver KS (the lesion disappeared after chemotherapy).

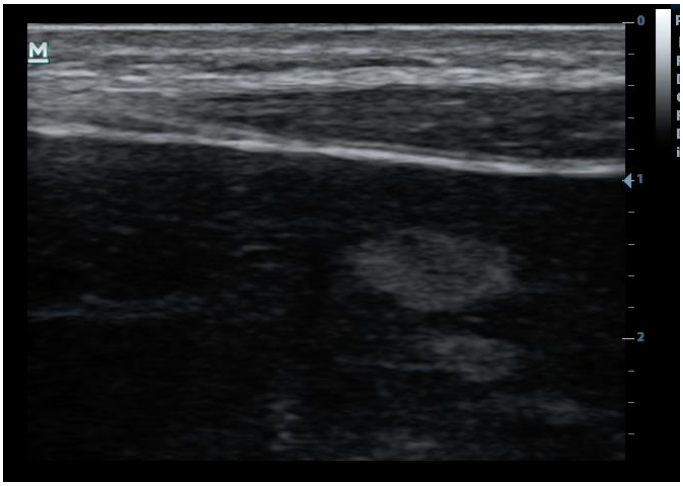

Small hyperechoic liver lesions are seen in disseminated MAC and *Pneumocystis jirovecii* infections. Bacillary peliosis or bacillary angiomatosis is characterised by cystic, blood-filled vasoproliferative lesions and spaces in the liver. This is linked to opportunistic infection with *Bartonella henselae* and has a sonographic appearance of multiple heterogeneous, more often hyper- but sometimes also hypoechoic, hypervascular focal liver lesions [Figure 8] [(28)]. Multiple, diffuse small echogenic lesions in the liver or spleen are seen as a 'snowstorm pattern'. Although this was initially described with *Pneumocystis jirovecii* infections [(11)], other organisms such as *Candida* and *Aspergillus* can be a cause. Histological features include foci of calcification, but their frequency is not sufficient to explain the multiple echogenic foci. The interfaces caused by the fibrosis could be largely responsible for the snowstorm appearance [(29)]. Ultrasound guided biopsy is used to determine the diagnosis [(12, 30)].

Hepatocellular carcinoma (HCC) is a common cancer in HIV-positive patients, mainly driven by hepatitis C virus co-infection. A focal lesion in a cirrhotic liver is highly suggestive of HCC [Figure 9]. The lesions are mostly hypoechoic, but hyperechoic lesions also occur especially if small. A mosaic pattern is typical, but rare [(31)]. Biannual ultrasound screening is

recommended for all patients with cirrhosis and those who are infected with hepatitis C with additional risk factors (family history of HCC, Asians and Africans) [(32, 33)]. Recent evidence suggests that more frequent screening may be beneficial in cirrhotic patients with HIV, in particular those with a detectable HIV viral load [(34)].

In patients at risk of HCC, the Liver Imaging Reporting and Data System (LI-RADS) can be used for classification. The American College of Radiology introduced LI-RADS to standardise the reporting and data collection of CT, MR and US imaging for hepatocellular carcinoma (HCC) [(35-37)]. LI-RADS is an algorithm which categorises observations from LR-1, a definitely benign lesion through to LR-5, reflecting a confident diagnosis of HCC. LR-M suggests a malignant lesion without specificity for HCC and LR–V suggests tumour thrombus in the portal vein. Between LR-1 and LR-5 are all the other possible observations reflecting the process of carcinogenesis including LR-2, a probably benign observation, LR-3 an observation of intermediate probability for HCC and LR-4, a highly suspicious observation for HCC. The categories LR-3 to LR-5 tend to roughly reflect the progression from large regenerative nodules (>4 mm) to mature HCC, paralleled by a derangement of intratumoural vascularisation.

Figure 8 **Bacillary angiomatosis linked to opportunistic infection with *Bartonella henselae* has a sonographic appearance similar to liver cirrhosis or nodular regenerative hyperplasia with multiple iso- or hyperechogenic focal liver lesions [(28)]. Gallbladder (GB); Portal vein branch (PV).**

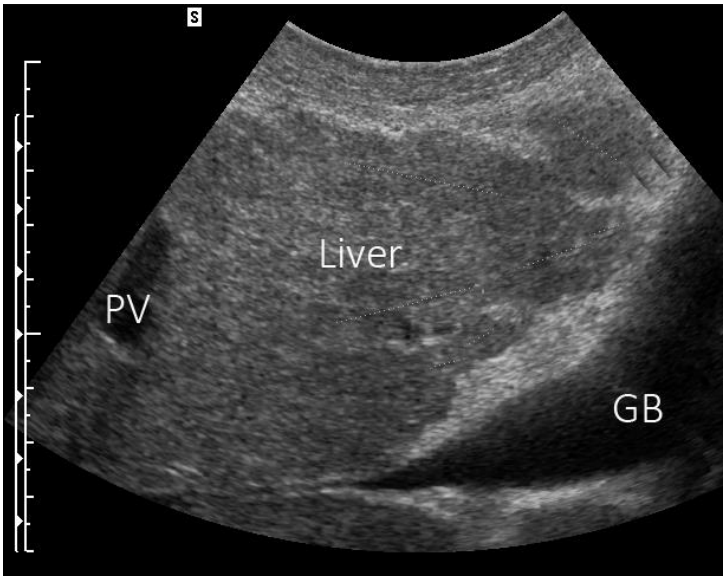

Figure 9 **Focal lesion in the cirrhotic liver of a patient infected with HIV and hepatitis B virus: liver HCC (biopsy result).**

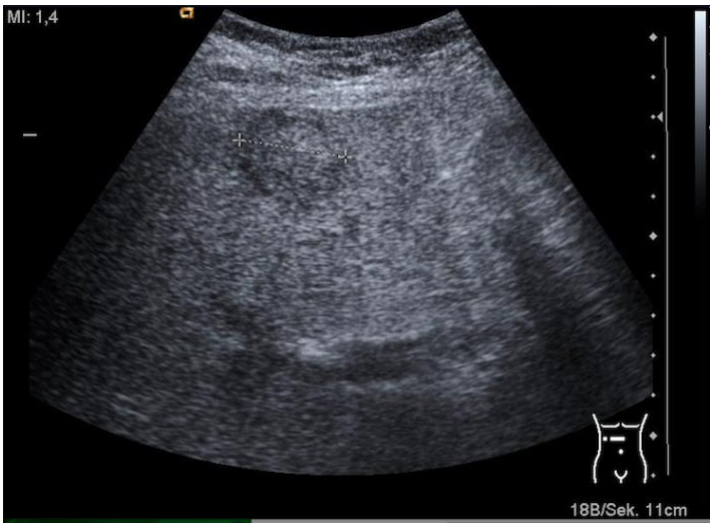

Incidental findings of benign focal liver lesions are found with the same frequency as the general population [(38)]. Contrast enhanced ultrasound (CEUS) is helpful in determining the nature of such lesions [(39)].

Gallbladder and bile ducts

Gallbladder wall thickening is a frequent finding in patients with HIV; however, in the majority of patients this is an incidental finding. A thick-walled and distended gall bladder, which shows the 'sonographic Murphy's sign' (tenderness on applying pressure with the probe in the gallbladder area), may point to cholecystitis. In contrast to immune-competent individuals, this may develop in the absence of gallstones ('acalculous cholecystitis') in patients with HIV [Figure 10]. Gallbladder thickening is a short-lived sonographic phenomenon of early phase acute hepatitis in approximately 50% of patients [(40)]. This must not be confused with acute cholecystitis where there is circumscribed pain on palpation.

Figure 10 Gallbladder thickening in emphysematous cholecystitis in an HIV-positive patient. A small gas bubble within the wall is indicated by the arrow.

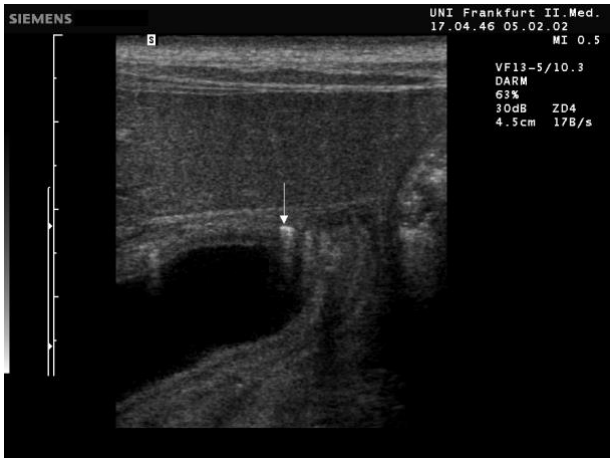

AIDS cholangiopathy is described in HIV patients with advanced immune suppression. It results from strictures in the biliary ducts due to opportunistic infections. On ultrasound it is characterised by irregular or smooth dilatation of intrahepatic bile ducts and concentric

thickening of the intra- and extrahepatic biliary tree (sclerosing cholangitis). Extrahepatic strictures, as well as papillary stenosis, have also been described. *Cryptosporidium parvum* is the most common pathogen associated with AIDS cholangiopathy [(41)].

Spleen

Splenomegaly is found in about a third of patients with AIDS in Africa [(15)]. This can be a non-specific finding due to the underlying HIV infection or due to other prevalent tropical infections like chronic malaria and schistosomiasis. It can also be a sign of diffuse hypoechoic infiltration, *e.g.* lymphoma [(18, 42)].

Focal splenic lesions can be due to infections such as pyogenic abscesses (generally hypoechoic), mycobacterial microabscesses (hypoechoic) [Figure 11] or toxoplasmosis (calcifications of a few millimetres in size with comet tail artefacts or a posterior acoustic shadow) [(43)]. A snowstorm pattern associated with *Pneumocystis jirovecii* pneumonia (PJP) and other opportunistic infections has also been described (see also the liver section) [Figure 12].

Figure 11 Tuberculosis of the spleen with small hypoechoic lesions in an HIV-positive patient. Similar images can be seen in other infectious (bacterial, fungal) diseases, haemophagocytosis-syndrome and lymphoma.

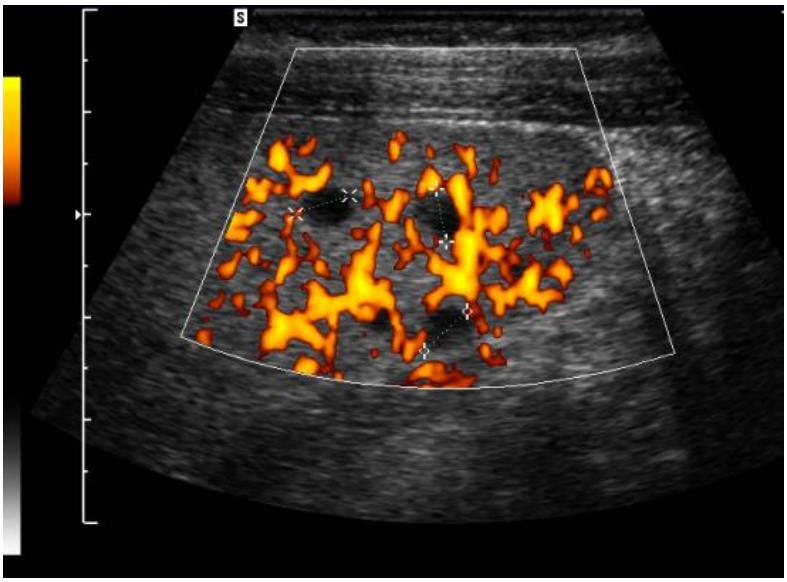

Figure 12 'Snowstorm' or 'starry-sky' pattern of the spleen with small hyperechoic lesions in an HIV-positive patient. *Pneumocystis jirovecii* pneumonia was deemed a possible cause (spleen histology not obtained).

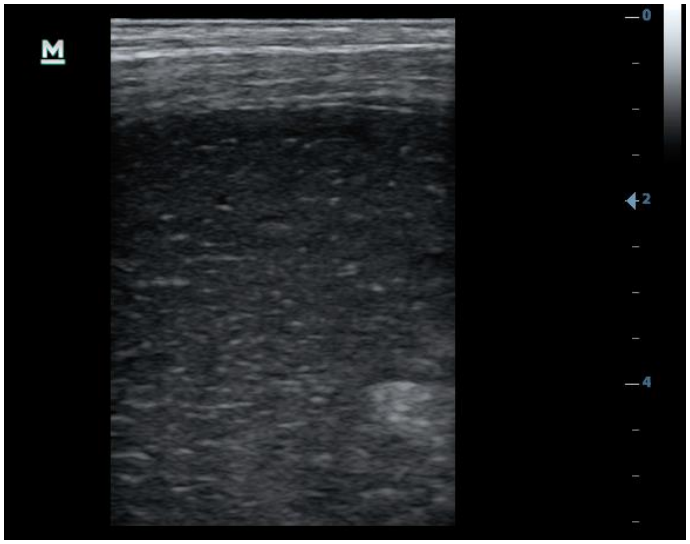

The most frequent neoplastic focal lesions of the spleen are a variety of lymphomas, which are commonly hypoechoic, ill-defined lesions of varying sizes [Figure 13]. Contrast enhanced ultrasound is helpful in delineating small infiltrations including haemophagocytosis lesions [(44)] and extramedullary haematopoiesis [Figure 14]. Burkitt's lymphoma lesions tend to be larger and may have a complex echo-structure [(11, 18)]. KS tends to be echogenic and may vary in size from a few millimetres to a large lesion occupying a large area of the spleen. A large variety of differential diagnoses have to be considered [(18, 42, 45)].

Figure 13 Multiple hypoechoic lesions of the spleen in an HIV-positive patient with lymphoma (NHL).

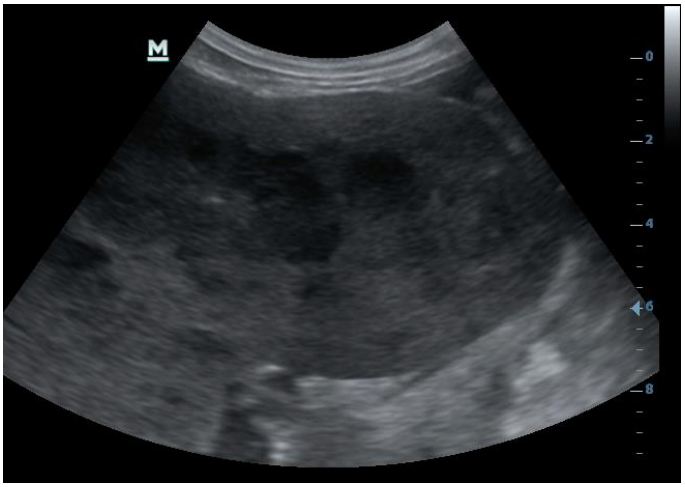

Figure 14 Extramedullary haematopoiesis. Extramedullary haematopoiesis can be seen in a variety of neoplastic and infectious diseases in association with HIV-infection.

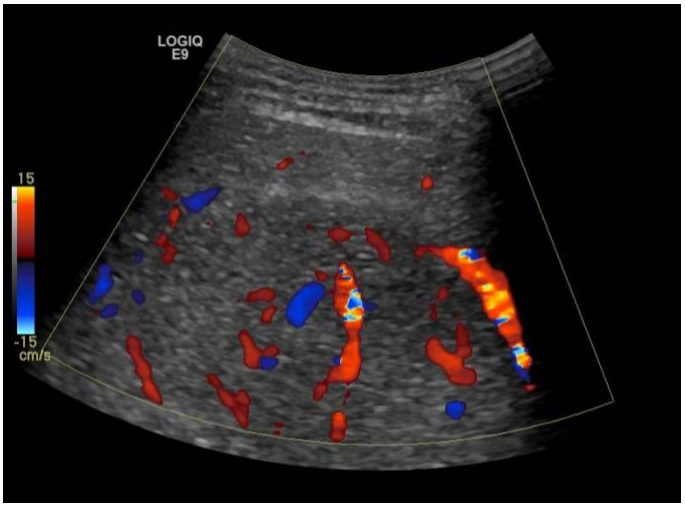

Pancreas

Although pancreatic involvement is frequently found in patients with HIV, it is rarely symptomatic and is usually in the context of disseminated infections. Pancreatitis may be seen secondary topancreatic duct strictures induced by opportunistic infections, similar to

the cholangitic changes already described. Tuberculosis of the pancreas rarely occurs in isolation. On ultrasound tuberculosis infiltration may be diffuse or circumscribed [Figure 15] [(46)]. In addition, focal masses of the pancreatic head due to tuberculosis or primary pancreatic lymphoma may cause obstruction of the pancreatic duct leading to secondary pancreatitis. Autoimmune pancreatitis can have similar characteristics on conventional ultrasound and is an important differential diagnosis [(47)]. CEUS and elastography are helpful to differentiate between different causes of pancreatic masses [(46)].

Figure 15 **Tuberculosis of the pancreas. Ductal adenocarcinoma was suspected by computed tomography. Ultrasound-guided biopsy revealed the final diagnosis of tuberculosis of the head of the pancreas. Endoscopic ultrasound elastography revealed softer tissue whereas in the more advanced stages harder elasticity is predominant [(48)].**

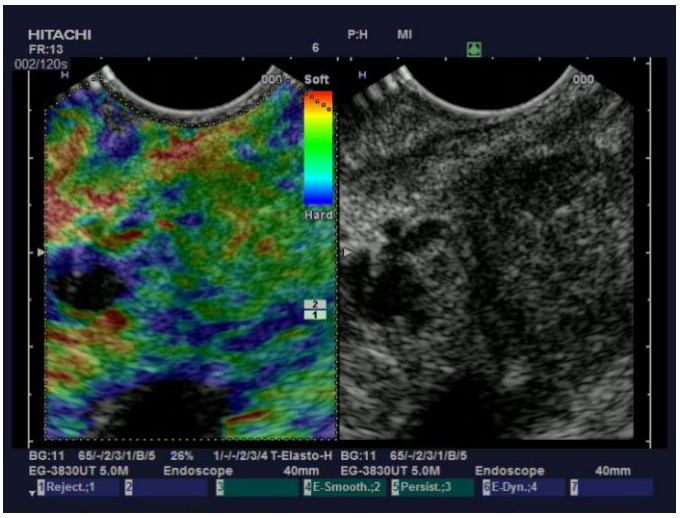

Gastrointestinal tract

The gastrointestinal tract is particularly prone to opportunistic infections owing to its large surface area and the presence of lymphoid tissue in the bowel wall. Inhomogeneous masses may be observed, but commonly pathology presents as a thickened (up to 2 cm), hypoechoic bowel wall similar to that seen in colitis [Figure 16]. Often a central hyperechoic, gas-containing lumen is visible (‘target sign’). Again, there is a wide differential diagnosis,

including opportunistic infections and neoplasms [(49)]. Endoscopy may be used to obtain diagnostic tissue samples, but because of the submucosal location of the lesions this does not always provide a diagnosis. Percutaneous ultrasound-guided biopsy of the bowel wall has also shown to be a safe way to obtain tissue samples [(50)].

Figure 16 Thickened stomach wall in an HIV-positive patient with disseminated Kaposi's sarcoma (histology on gastroscopy biopsy confirmed KS).

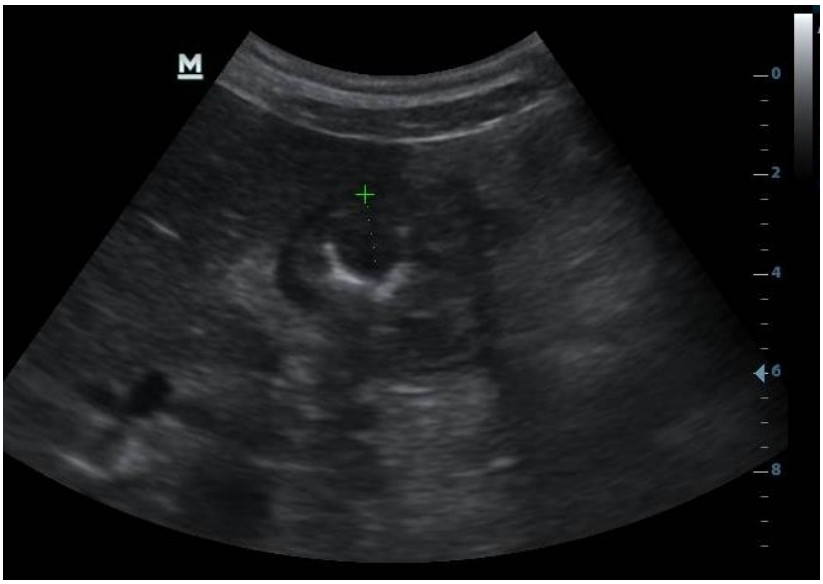

Ascites

Ascites is a relatively common finding that is encountered in up to 1 in 5 patients with AIDS in some African studies [(15)]. Ascites may be due to portal hypertension, especially in co-infected patients (with hepatitis C or B virus) or those with alcoholic liver disease. Exudates may be due to infections or tumours and numerous causes have been described. Ultrasound helps to identify even small amounts of intraperitoneal fluid and can assist with paracentesis. Microbiological culture and PCR (polymerase chain reaction) may yield results of *Mycobacterium tuberculosis*, *Mycobacterium avium* complex (MAC) and CMV, but in rare cases organisms such as *Candida albicans*, *Cocciodiodes immitis, Pneumocystis jirovecii, Toxoplasma gondii* and *Encephalitozoon cuniculi* have been found.

Malignant ascites is seen less frequently and should be suspected in culture-negative exudative peritoneal fluid. KS and lymphoma are the most common causes in HIV-positive patients with advanced immune suppression. Primary effusion lymphoma associated with human herpes virus 8 (HHV-8) is a rare, aggressive mature B-cell neoplasm predominantly observed in patients with HIV. It usually manifests with effusions in the pleural, pericardial or peritoneal space [(51)]. Several mechanisms associated with HIV infection, as well as traditional risk factors including age, opportunistic infections and lifestyle choices, may increase the risk of venous thromboembolism in patients with HIV [(52)]. Therefore, portal vein thrombosis is another cause of ascites that should be suspected and can be demonstrated with Doppler ultrasound.

Kidney

Patients with HIV have an increased incidence and prevalence of acute and chronic renal failure. While common causes of chronic renal failure also occur in patients with HIV, the most common HIV related disease is HIV associated nephropathy (HIVAN), histologically characterised by focal-segmental glomerulosclerosis. This is the most frequent renal pathology found on ultrasound. The kidneys are typically normal or increased in size and the parenchyma is hyperechoic [Figure 17]. This appearance is non-specific and can be seen in other renal diseases such as diabetic glomerulosclerosis or other forms of chronic glomerulonephritis. This sonographic finding should prompt an assessment for proteinuria. In some cases renal biopsy may be indicated to determine the exact diagnosis.

Figure 17 Hyperechogenic (compared with adjacent liver tissue) kidney in a patient with HIV associated nephropathy (HIVAN) .

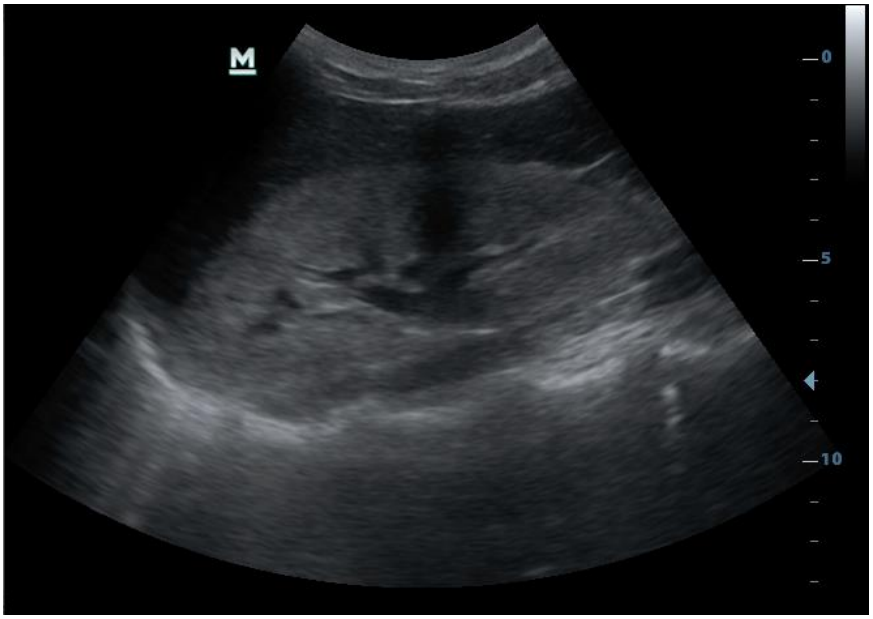

Nephrocalcinosis with circumscribed renal calcifications can be seen in generalised MAC and histoplasmosis infections, as well as in patients taking medication such as sulfadiazine, acyclovir and in particular indinavir, which can induce renal stone-like crystal aggregates. Abscess formation is typical in tuberculosis. Retroperitoneal masses like lymphadenopathy can obstruct the ureters and result in hydronephrosis [(53)].

Chest ultrasound

Lung ultrasound

Pulmonary diseases are common in HIV-positive patients. Opportunistic infections, neoplastic diseases and other pulmonary pathology occur more frequently than in HIV-negative individuals [(54)]. The differential diagnosis of pulmonary disease in HIV-positive patients is broad and ultrasound may function as an adjunct imaging modality [(55)]. Its use in the diagnosis of tuberculosis is described in the section on TB. In HIV-positive patients with PJP, B-lines, subpleural consolidations and cystic changes are described [(56)]. The hyperechoic cystic changes seem to be particularly suggestive of PJP [(57)]. Lung

consolidation with air bronchograms and pleural effusion should prompt suspicion of other aetiologies (e.g. bacterial pneumonia, TB).

Heart

HIV-associated cardiomyopathy is reported in 9–57% of patients who are HIV-positive in Africa [(58)]. Variation in study design, population and a lack of a clear definition for cardiomyopathy may account for this wide range. There is limited data on the pathogenesis of cardiomyopathy in HIV-infected individuals in Africa [(58)]. A study from the Democratic Republic of Congo reported cardiac histology from 16 patients, all of which had histopathological evidence of myocarditis. *Toxoplasma gondii w*as found to be the cause in 3 patients (18.75%), *Cryptococcus neoformans* in another 3 (18.75%) and *Mycobacterium avium intracellulare* in 2 (12.5%) [(59)]. Direct HIV-associated cardiac inflammation was considered to be the cause in the remainder (50%). These aetiologies are different from the cardiotropic viruses seen more frequently in developed countries. There seems to be a relationship between the degree of immunosuppression and the likelihood of cardiomyopathy [(60, 61)]; antiretroviral therapy prevents immunosuppression, but it is unclear whether it reverses cardiomyopathy. Abdominal sonographic views may show a typically enlarged, dilated ventricle (diastolic diameter of more than 5.5 cm) with globally reduced contractility; this may prompt further investigation by echocardiography. Pericardial effusions are also a common finding in HIV infected patients. TB pericarditis will be discussed in detail in the section on TB. Malignancy, in particular KS, is an important differential diagnosis.

Other ultrasound applications

Lymph nodes

Enlarged lymph nodes are frequently seen in patients with HIV and have a wide differential diagnosis. Intra-abdominal lymph nodes larger than 1.5 cm are commonly considered pathological and are often round and plump and can occasionally become very large [Figure 18].

Figure 18 Enlarged lymph nodes encasing the coeliac axis, common hepatic artery and splenic artery (transverse section).

Often the nodes appear hypoechoic and have a disrupted architecture with absence of the 'hilum fat sign' and sometimes, liquid, necrotic areas. The differential diagnosis of enlarged lymph nodes in HIV-positive patients includes tuberculosis, MAC, toxoplasmosis, CMV, as well as generalised KS and lymphoma. Castleman disease is another lymphoproliferative disease associated with HHV-8 in HIV-positive patients presenting with fever and lymphadenopathy.

Ultrasound-guided needle biopsy can often help make a diagnosis. The use of ultrasound for the differential diagnosis of enlarged lymph nodes has been extensively published, including conventional ultrasound [(53, 62)], contrast enhanced ultrasound [(62-65)] and elastography [(66, 67)].

Parotid gland

5–10% of patients with HIV-1 infection have parotid swellings, most commonly due to cystic lymphoepithelial lesions of the salivary gland. Sonographic examination shows unilaterally or bilaterally enlarged glands with cystic lesions [Figure 19]. The size of the sonolucent areas may vary from a few millimetres to a few centimetres, cyst numbers vary from a single cyst

to numerous cysts and represent lymphoepithelial cysts, intraparotid lymphadenopathies and parenchymal lymphoproliferation [(68)].

Figure 19 Multiple hypo- to anechoic lesions in the parotid gland of an HIV-positive patient: diffuse infiltrative lymphocytosis syndrome.

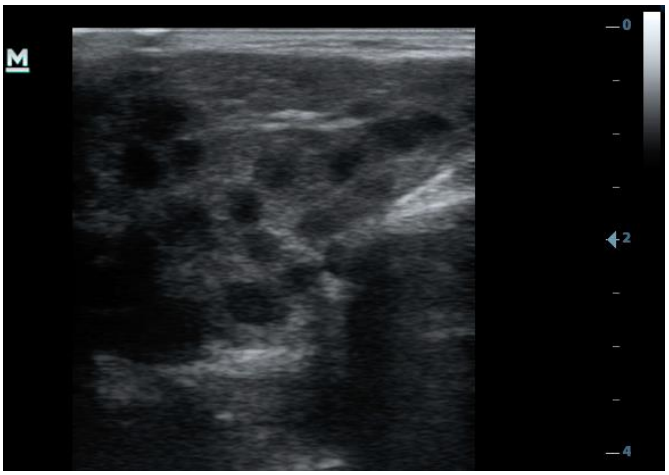

If necessary, the diagnosis can be confirmed through fine-needle aspiration. Treatment includes simple aspiration, surgical resection or radiotherapy; most cases that are treated with antiretroviral therapy show regression.

Tuberculosis (TB)

Introduction

Infections with *Mycobacterium tuberculosis* commonly affect the lungs and are often diagnosed by a chest radiograph as well as by sputum microscopy (acid-fast bacilli (AFB)), PCR or sputum culture. Nevertheless, because TB is a systemic disease [(69)], extrapulmonary manifestations are seen regularly and in cases of concomitant HIV infection they are even more frequent. In a significant proportion of HIV-positive patients with suspected TB, ultrasound can identify findings suggestive of TB despite a normal chest radiograph [(70)]. As material for microscopy and culture is not readily obtainable in extrapulmonary tuberculosis (EPTB), diagnosis often depends on aspiration of suspicious

fluids or lymph nodes, or alternatively the diagnosis is made based on clinical criteria alone in high prevalence settings. The highly suggestive combination of effusions, enlarged lymph nodes and focal lesions in the spleen and liver is well described as suggestive of TB in various settings. In rural South Africa, where there is an extremely high prevalence of HIV and TB and low resources for further diagnostic work-up, the findings may be considered sufficiently specific to initiate anti-TB treatment. In a case series of high-risk patients from an Italian cohort, these findings were replicated and the diagnosis of tuberculosis was confirmed by ultrasound-guided biopsy [(71)]. Similar patterns of ultrasound findings were described in patients in other African settings [(72-74)], Asia [(75-77)], the Middle East [(78)] as well as in patients from low prevalence settings in Europe [(79)]. Once a clinical diagnosis is made, standard treatment for all forms of EPTB is similar to that of pulmonary tuberculosis; usually 4 antibiotics (rifampicin, isoniazid, ethambutol and pyrazinamide) are given for 2 months followed by 4 months of rifampicin and isoniazid. This section of the chapter will discuss the ultrasound findings of TB, often seen in HIV-positive patients but also in HIV-negative individuals.

Abdominal ultrasound

Liver

Involvement of the liver in TB is common (up to 80% in EPTB), however clinical manifestations of this involvement are not frequently seen [(80)]. Sonographically, two main forms of involvement are seen. An enlarged liver with a homogeneous, bright echo-pattern points towards diffuse hepatic granulomatous disease (often wrongly described as granulomatous hepatitis; as liver cells are unaffected ‘hepatic granulomatous disease’ would be more correct) [Figure 20] [(81)]. The diagnosis is reached by ultrasound-guided liver biopsy. The other form manifests as focal liver lesion(s).

Figure 20 Echogenic liver in granulomatous hepatic disease caused by TB (proven by biopsy).

Focal tuberculomas present as ‘abscess-like’ masses, which are usually hypoechoic or of mixed echogenicity. They may be single or multiple and vary in size from 0.5–12 cm [Figures 21] [(82)].

Figure 21 Tuberculosis of the liver with granulomatous infiltration of the liver parenchyma and bile ducts (in between markers).

A very rare form of hepatic involvement is ‘serohepatic tuberculosis’ characterised by predominant involvement of the serosal plane and lesions centred in the subcapsular area of the liver. The thickened liver capsule and sub-capsule overlying these hypoattenuating lesions resemble ‘sugar-coating’, an appearance popularly referred to as ‘frosted liver’ [(83)]. The appearance of hepatic TB on CEUS often shows the size of the lesions to be larger than in conventional ultrasound. During the arterial phase, approximately half of the lesions show a rapidly and markedly enhancing rim with a hypoenhanced centre; others show transient enhancement of the whole lesion with uneven intensity. Histopathological analysis shows that the enhanced rim is due to inflammatory hyperaemia in the normal hepatic sinusoid. During the portal phase, most lesions showed distinct wash-out of the contrast agent in the centre and maintained a hypoechoic appearance. Histopathological analysis show that the wash-out in the centre corresponds to the destruction of the hepatic sinusoid with inflammatory granulation [(84)]. Due to the differential diagnosis of malignancy, biopsy is often required.

Tuberculosis infection may present with an enormous heterogeneity of manifestations. It should be noted that all the hepatic lesions (as well as all tuberculous lesions in general) can initially increase in size during successful treatment as the improved immunological response increases the inflammatory reaction. This does not suggest treatment failure and it should be followed up.

Disseminated abdominal infection (lymph nodes and spleen)

Disseminated abdominal TB affecting mainly abdominal lymph nodes and the spleen is a pattern frequently seen in HIV-positive patients especially in those with low CD4 counts, but the pattern can also found in HIV-negative individuals. Clinical signs and symptoms are usually weight loss, diffuse abdominal pain and possibly diarrhoea [(85)].

Abdominal lymph node enlargement and ascites are the most common findings and hypoechoic lesions of the spleen are seen in about 50% of patients [Figure 22] [(85)]. Although the signs are not completely specific, lymph nodes are larger in TB patients than in patients with non-tuberculous mycobacteria (NTM) [(86)]. Additionally, TB nodes more frequently show darker, ‘anechoic’ areas within the nodes whereas NTM nodes tend to be more uniform.

The splenic microabscesses represent a ‘miliary’ pattern of infection, although many patients show no miliary pattern on a chest radiograph [(70)]. Up to 25% of the patients who are found to have sonographic signs of disseminated TB do not have features suggestive of TB on the chest X-ray. As the splenic lesions are often very small and sometimes differ only slightly in echogenicity from the surrounding tissue, the use of a linear transducer is essential. The splenic hypoechogenic foci are suggestive of *Mycobacterium tuberculosis* infection rather than non-tuberculous mycobacteria (NTM), as they are rarely seen in the latter [(87)]. Alternative differential diagnoses of multiple small (<1 cm) splenic lesions are Bartonella infections (peliosis), visceral leishmaniasis, melioidosis (in patients from Southeast Asia) and disseminated brucellosis [(88)]. Tuberculous abscesses in the spleen may present as a large solitary lesion or as multiple lesions, the latter raising the possibility of an alternative diagnosis such as malignancy (e.g. lymphoma). If CEUS is available, malignant lesions tend to show hypoenhancement in the arterial phase and hypoenhancement in the parenchymal phase. Benign lesions, including TB tend to show isoenhancement or hyperenhancement in the arterial phase and isoenhancement or hyperenhancement in the parenchymal phase [(89)]. Biopsy of the splenic lesion may be indicated. Fine needle aspiration biopsy (FNAB) is infrequently done because the risk of haemorrhage is considered high, but studies have shown that complications are less frequent than perceived and FNAB (e.g. with a 22 G spinal needle) can often yield diagnostic material [(90)].

The sonographic findings of disseminated TB, for example enlarged lymph nodes and splenic lesions, but also pleural and pericardial effusions, tend to disappear within 3 months of effective TB treatment irrespective of HIV status. In one case series, persistent findings beyond this period were due to non-compliance with drug therapy, multidrug-resistant TB, an alternative diagnosis or immune reconstitution inflammatory syndrome (IRIS) [(91)].

Figure 22 Hypoechogenic tuberculous nodules seen with a linear probe.

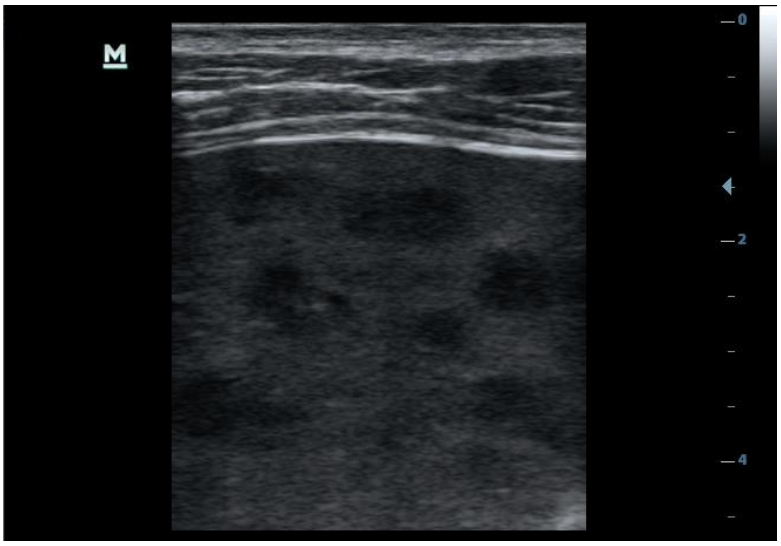

Pancreas

Features of tuberculosis in the pancreas are described in the previous section on ultrasound in HIV patients. In summary, a focal lesion in the pancreas can be a sign of tuberculosis [Figure 15].

Gastrointestinal tract

Although tuberculosis can involve any region of the gastrointestinal tract, it most frequently affects the ileocaecal valve, the adjacent ileum and the right-sided colon [(17, 92-95)]. The common sonographic appearance is of an asymmetric thickened bowel wall, possibly with intramural abscesses [Figure 23] and fistulae [Figure 24]. A ‘white bowel’ has been described [Figure 25] as well as hypoechoic oedema of Kerckring's folds with mesenteric thrombosis [(17)]. Extra-intestinal signs like enlarged mesenteric lymph nodes and mesenteric thickening are frequent accompanying findings [(17)]. Patterns of contrast enhancement in CEUS have been described for intestinal TB [(96)] but their diagnostic value remains to be determined.

Figure 23 Gastrointestinal tuberculosis in an HIV-positive patient with intramural abscess formation in between markers.

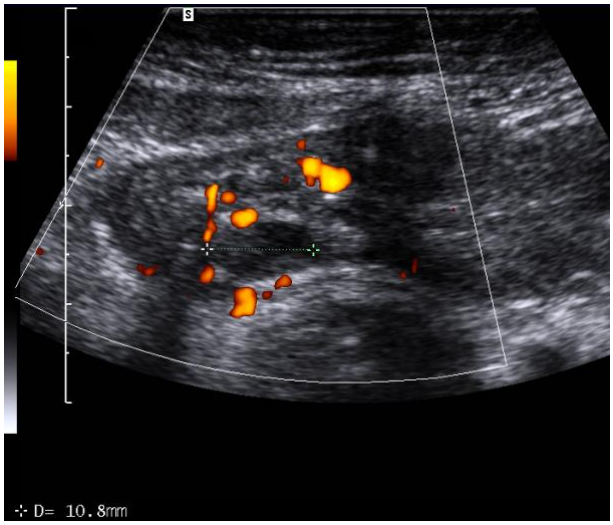

Figure 24 Gastrointestinal tuberculosis in an HIV-positive patient with complex infiltration, a fistula (arrow) and abscess (ABS) formation (panoramic imaging).

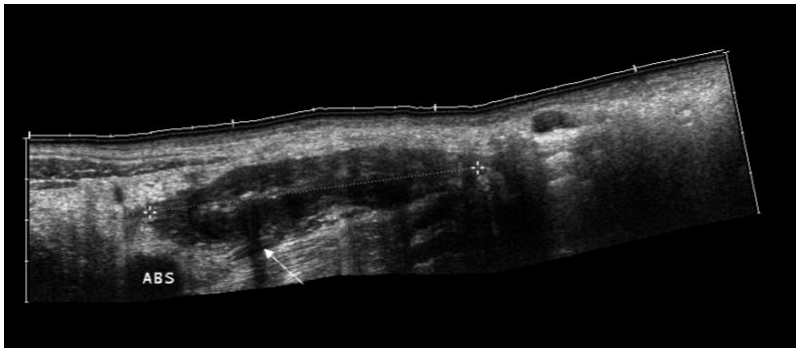

Figure 25 Gastrointestinal tuberculosis in an HIV-positive patient with complex inflammation of the lymphatic vessels resulting in so-called white bowel. Appendix (APP); caecum (COE); terminal ileum (TI).

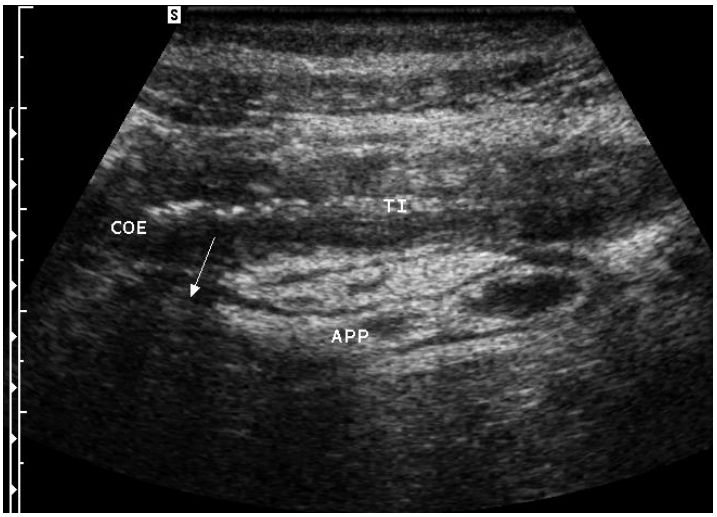

Peritonitis

TB peritonitis is probably caused by haematogenous spread and reactivation of long-latent foci or mesenteric lymph nodes [(97)], but contiguous spread from the bowel or fallopian tubes is also possible. Ultrasound findings are (a) ascites (clear or complex with fixed membranes, septae, strands and floating debris), (b) thickened parietal peritoneum possibly with nodules [Figure 26], (c) omental thickening (‘omental cake’) and thickening of the mesentery and (d) abdominal lymphadenopathy [(98)].

Figure 26 Circumscribed peritoneal thickening in an HIV-positive patient with peritoneal tuberculosis.

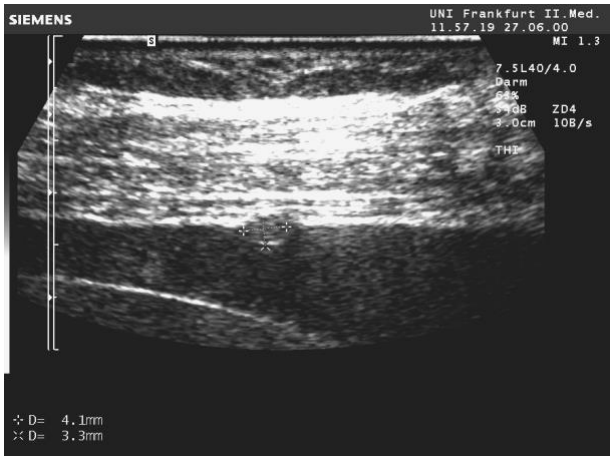

Ascites is usually straw-coloured or sometimes (10% of cases) blood stained, the protein content is usually more than 2.5 g/dl and leucocytes with lymphocytic predominance can be seen. Direct microscopy is usually AFB negative as the bacterial load is low and mycobacterial cultures of ascites are also frequently negative. Reported sensitivity of the Xpert MTB/RIF assay compared with the culture varies between 19% and 71%; specificity is high at 100% [(99, 100)]. Due to the low sensitivity, negative test results in ascites cannot be considered diagnostic. Biopsies of pathological peritoneal and omental lesions offer an alternative method to obtain a diagnosis. When patients show sonographic abnormalities of the peritoneum or greater omentum (diffuse thickening), ultrasound-guided percutaneous biopsies using Tru-Cut needles can frequently determine the aetiology [(101)]. Laparoscopy can detect peritoneal lesions and allow biopsies to be obtained from various parts of peritoneal lesions but is more invasive and rarely available in the resource-limited setting. 'Blind' peritoneal biopsy using forward-biting endoscopy biopsy forceps has been successfully used as an alternative [(102)].

Renal and urinary tract

Genitourinary TB (GUTB) is seen more frequently in male than in female patients and about a third of the patients report previous tuberculosis [(103)]. The pathogenesis involves the haematogenous spread of *Mycobacterium tuberculosis* followed by seeding in the renal

cortex in which a high oxygen tension exists. During reactivation, granulomas form that spread into the medulla and can lead to necrosis of renal papillae and renal obstruction may occur. Bacilluria can lead to ureter and bladder involvement with fibrosis and reflux. The most common symptoms are storage symptoms, dysuria, lumbar pain and haematuria. Only one in five patients complain of systemic symptoms like fever and malaise [(103)].

Sonography may show renal calcifications, papillary irregularities and intrarenal masses [Figure 27].

Figure 27 Renal tuberculosis in HIV-positive patients. The infiltration patterns vary from larger abscesses (a, b) to tiny infiltration (c). Contrast enhanced ultrasound is helpful in delineating non-vascularised abscesses (b) [(104)]. Cortex of the kidney (Nierenrinde).

a

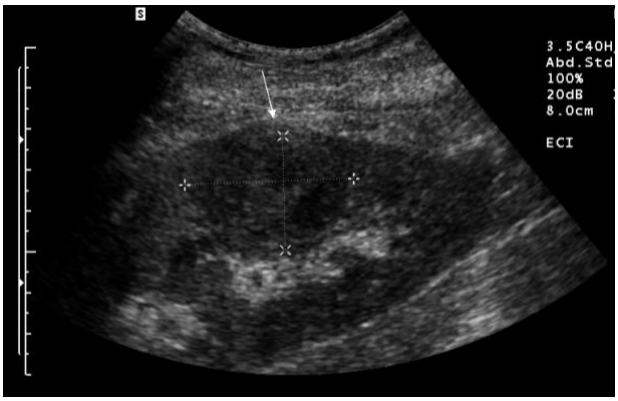

b

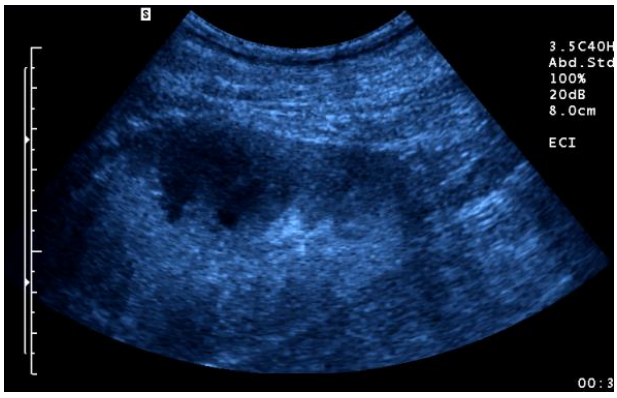

c

Hydronephrosis due to strictures, thickening and dilatation of the ureter and bladder abnormalities (wall thickening and masses) may also be seen [(105)]. The diagnosis is usually made with a urine culture; urine specimens can also be assessed by GeneXpert MTB/RIF, a recent meta-analysis showed good sensitivity (87%) and specificity (91%) [(106)].

Scrotal involvement in the form of swelling due to 'cold abscesses' in the epididymis and testis is well described [(107)]. Focal areas of decreased echogenicity can be demonstrated on ultrasound. Differentiation from tumours may be difficult, so image-guided aspiration is often needed.

Women with GUTB can present with menstrual irregularity, infertility, abdominal pain and pelvic inflammatory disease [(107)]. Most patients have abnormal hysterosalpingograms with endometrial adhesions, fallopian tube obstruction and small calcifications in the adnexal area. Ultrasound may show tubo-ovarian abscesses, extension of these collections to extraperitoneal areas can suggest TB, so often the diagnosis is made by aspiration and microbiological analysis of the material [(108)]. Adnexal masses due to TB are frequently misdiagnosed as ovarian cancer and are only correctly diagnosed after laparoscopy. It is important to remember that ovarian TB can be associated with elevated CA 125 levels, a tumour marker for ovarian cancer [(109)]. Checking CA 125 levels at follow-up may even be useful to assess the therapeutic response to TB treatment [(110)].

Chest ultrasound

Lung

The role of ultrasound has become established in recent years since the introduction of the BLUE protocol, especially in acute medicine and intensive care [(111)]. Although ultrasound signs are non-specific, chest ultrasound appears to be a useful, complementary and low-cost tool, which explains the growing interest in applying the technique to patients with TB. The main features of pulmonary tuberculosis (PTB) are focal opacities and collapsed lung segments or lobes, which are of course indistinguishable from other (bacterial) pneumonias [(55)]. In patients with miliary TB, multiple B-lines and comet-tail artefacts disseminated throughout multiple lung areas, as well as a pattern of sub-pleural granularity, have been described [(112)]. In a recent study, subpleural nodules were described which were mostly multiple and also found in radiologically normal areas of the lung. Other findings were lung consolidation, the previously described miliary patterns made up of miniature nodules and pleural and pericardial effusions [(113)]. When tuberculomas are located in the pleura, they can be visualised by ultrasound. Investigations using CEUS show rim enhancement, homogeneous or heterogeneous enhancement. Enhancement patterns of these juxtapleural pulmonary tuberculomas correlate well with their pathological features; caseating necrotic areas do not enhance while granulomatous inflammatory areas show enhancement [(114)].

Pleuritis

The pleura may be affected by TB in different ways:

- Effusion that develops usually a few months after primary infection (hypersensitivity reaction).
- Effusion developing as a result of lung disease in older adults, which might develop into purulent effusion (empyema).
- Rupture of a cavity and escape of bacteria and air into the pleural space, from which an empyema and pyopneumothorax may result.
- Complicated miliary TB that result in polyserositis.

In the majority of patients the disease course is characterised by a subacute onset of fever, cough, pleuritic chest pain and breathlessness as the effusion evolves [(115)]. Tuberculous pleural disease is usually unilateral. In all of the above mentioned pleural pathologies, effusions can be observed sonographically and fibrin strands are often seen [Figure 28]. A lymphocyte-rich exudative pleural effusion with a 'complex septated pattern' (defined as 'presence of strands, hyperechoic lines within the effusions, floating inside the pleural space, weblike or branching') is seen more frequently in TB pleuritis than in effusions associated with lung cancer when compared to anechoic, homogeneously echogenic or complex non-septated patterns [(116)]. A complex septated sonographic pattern is also a sign that predicts residual pleural thickening after anti-TB treatment. Marked residual pleural thickening is associated with decreased lung volumes (i.e. forced vital capacity). Therefore, the initial sonographic features can predict sequelae of TB after treatment [(117)].

Figure 28 Complex pleural effusion with debris and fibrinous septae in a patient with HIV-associated TB.

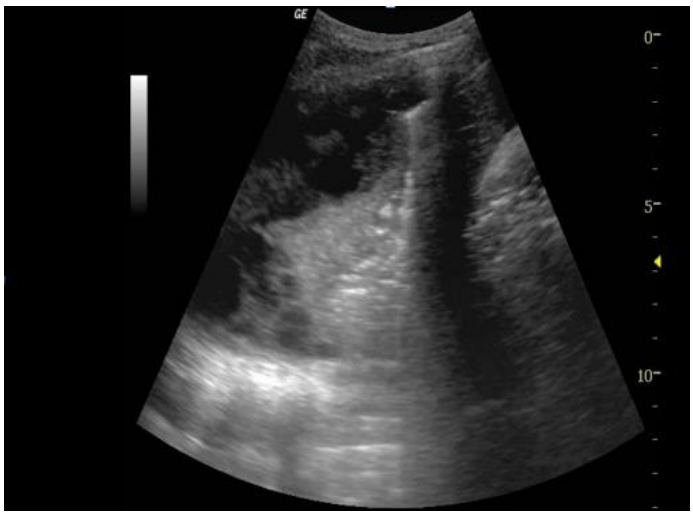

Ultrasound may be used to guide aspiration and if a total white blood cell count of >500 cell/mm^3 and protein >2.5 g/dL are found in the aspirate, an empyema can be diagnosed. This can be further differentiated clinically between a 'thin empyema' (possible to aspirate through a cannula) and a 'thick empyema' (which may need a transthoracic drain). If pleural

fluid is aspirated this can also be sent for TB-PCR. A recent meta-analysis reported the pooled sensitivity of GeneXpert MTB/RIF for pleural TB as 46.4% and the pooled specificity as 99.1% [(118)]. In cases of a negative test where TB is still suspected a blind pleural biopsy is usually the next diagnostic step. Ultrasound-assisted pleural biopsies performed with an Abrams needle were found to be more likely to contain pleura and have a significantly higher diagnostic sensitivity for pleural tuberculosis than Tru-Cut biopsies [(119)].

Mediastinum

Particularly in children, the use of ultrasound of the mediastinum through the suprasternal notch is an interesting option to identify enlarged lymph nodes in the upper mediastinum [Figure 29] [(120)]. Initial studies were very promising and the technique is well described [(121-123)]. Nevertheless, a recent study highlighted the difficulty of this method and image interpretation, a suboptimal interobserver agreement and the fact that the presence of enlarged lymph nodes per se was not useful for identifying PTB. The size of the detection of larger lymph nodes may be helpful in discriminating children with PTB from those with other respiratory diseases [(124)].

Figure 29 Enlarged mediastinal lymph nodes seen using the suprasternal notch acoustic window in a South African child with TB (a). Adjacent to the lymph nodes, the aortic arch is visible (b). (Courtesy of Dr. Sabine Belard, Charite-Berlin, Germany)

a

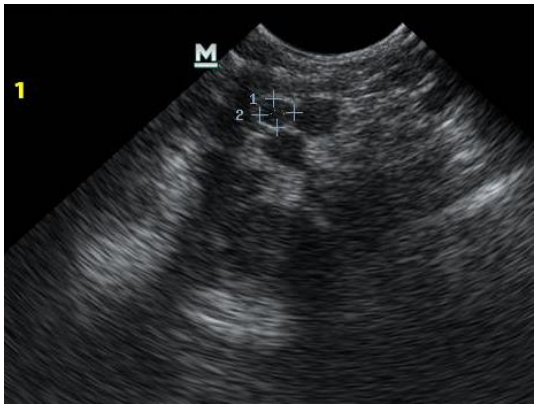

b

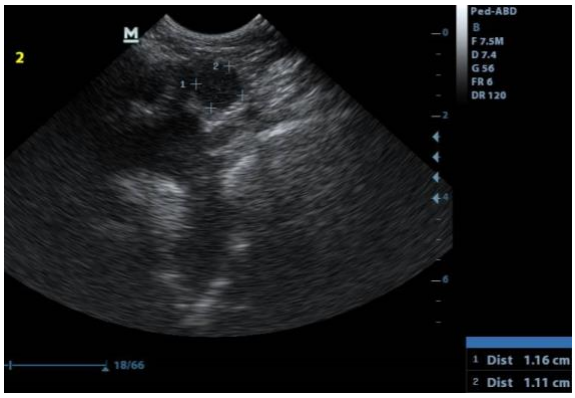

Heart (pericarditis)

TB pericarditis is one of the acutely life-threatening manifestations of EPTB owing to the risk of cardiac tamponade [(125)]. It is the most common cause of pericarditis in Africa. In a South African series, TB pericarditis accounted for up to 70% of the cases referred for diagnostic pericardiocentesis [(126)] [Figure 30].

Figure 30 Enlarged cardiac silhouette on a chest radiograph in tuberculous pericarditis.

TB pericarditis usually develops by retrograde lymphatic spread of *Mycobacterium tuberculosis* from peribronchial or mediastinal lymph nodes or by haematogenous spread from primary tuberculous infection [(127)]. The immune response to viable acid-fast bacilli

penetrating the pericardium is responsible for the associated morbidity. Non-specific signs and symptoms such as fever, night sweats and weight loss are observed and chest pain, cough and breathlessness are common. In African patients, chronic cardiac compression mimicking congestive heart failure is another common presentation [(128)].

Sonographically, two forms of pericardial disease secondary to TB can be differentiated: pericardial effusion and constrictive pericarditis. Pericardial effusions are characterised by a large, anechoic-rim around the heart. It is important to assess whether the effusion impairs the normal filling of the right ventricle or atrium as this would suggest cardiac tamponade [Figure 31]. A study looking at the usefulness of ultrasound findings in African inpatients with respect to therapeutic decisions found that pericardial effusions are one of the most relevant findings [(129)].

Figure 31 Pericardial effusion in an HIV-positive patient with pericardial TB.

Figure 32 Pericardial effusion with fibrinous material in an HIV-positive patient with pericardial TB.

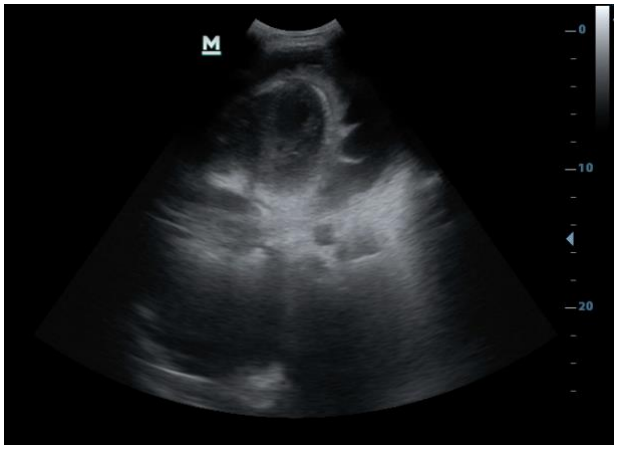

Often a thickened pericardium with fibrinous strands and exudative coating material are observed floating in the effusion [Figure 32]. If aspirated, the effusion is typically exudative and may yield positive results in mycobacterial culture or PCR [(127)]. Xpert-MTB/RIF is reported to have a sensitivity of 64% (52.4% to 75.1%) and a specificity 100% (85.6% to 100%) when used on pericardial fluid [(130)]. When TB pericarditis is suspected, sputum samples should be submitted at the same time for AFB and PCR.

In cases of constrictive pericarditis, a thick fibrinous exudate is seen in the pericardial sac [Figure 33], which is associated with reduced movement of the surface of the heart. The pericardial exudate condenses into a thick skin surrounding the heart and this can usually be distinguished from the myocardium [(127)].

Figure 33 Hypoechoic pericardial material surrounding the heart in a patient with constrictive pericarditis.

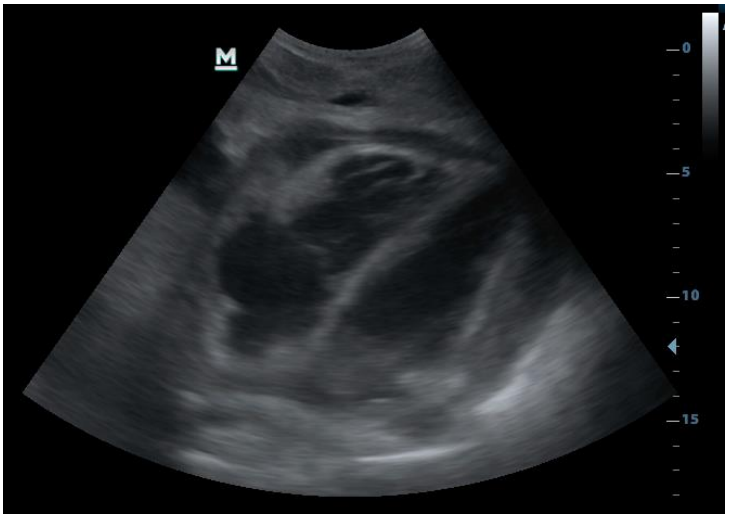

Corticosteroids may be given in addition to antibiotic treatment, although their impact on outcome is still controversial. A statistically non-significant, but potentially large reduction in mortality was observed in one randomised trial [(131)]. A recent multicentre study found that prednisolone had no significant effect on a composite outcome measure of death, cardiac tamponade requiring pericardiocentesis or constrictive pericarditis in patients with tuberculous pericarditis [(132)]. Prednisolone therapy on the other hand was associated with significant reductions in the incidence of constrictive pericarditis and hospitalisation.

As patients often experience faster clinical improvement we prescribe steroids for 6-8 weeks, especially in cases with cardiac tamponade, despite the fact that HIV-positive patients who receive steroids may have a small but significant increased risk of developing HIV-associated malignancies, primarily KS [(132)]. Colchicine, while generally effective for the treatment of acute and recurrent pericarditis, seems not to have a benefit in TB pericarditis [(133, 134)].

Other ultrasound applications

Lymph nodes

Enlarged lymph nodes are a frequent presentation of patients with TB, but they have a wide differential diagnosis, especially in patients with HIV in a tropical setting. The differential diagnosis includes tuberculosis, MAC, toxoplasmosis, CMV, as well as generalised KS and lymphoma. Castleman disease is another lymphoproliferative disease associated with HHV-8 in HIV-positive patients that presents with fever and lymphadenopathy [(135)]. As discussed above, in disseminated TB, intra-abdominal lymph nodes larger than 1.5 cm are commonly considered pathological, they are often round and plump and can occasionally become very large [Figure 18].

Peripheral lymphadenopathy most frequently involves the lymph nodes of the neck, but can also affect the axillary and inguinal nodes. The use of ultrasound for the differential diagnosis of enlarged lymph nodes has been extensively published, including conventional ultrasound [(53, 62, 136-138)]. On gray-scale sonography, TB nodes tend to be hypoechoic, round and without an echogenic hilum (‘hilum fat sign’). They may show intranodal cystic necrosis (‘caseating necrosis’). Often nodal matting and adjacent soft-tissue oedema is seen. On colour Doppler or power Doppler the vascular distribution in TB nodes is varied and can mimic benign or malignant nodes. However, displacement of hilar vascularity is common in TB nodes probably due to the intranodal cystic necrosis which displaces the vessels [(138)].

Elastography has been reported to give additional diagnostic information [(139, 140)], although it is mainly used to differentiate between benign and malignant nodes and it is not widely available in resource limited settings. CEUS is another modality that has been frequently investigated in the differential diagnosis of enlarged lymph nodes [(62-65, 141, 142)] and again, the price of the contrast agent is prohibitive in most settings where the highest number of TB patients are seen.

Ultrasound guided biopsy is a more practical way to reach a final diagnosis. Initially enlarged lymph nodes in suspected cases of TB can be aspirated with a fine needle, the aspirate can be flushed into a small amount of normal saline and the sample submitted for GeneXpert MTB/RIF [(143, 144)]. The test is easy to perform, widely available and specific and is more sensitive than smear microscopy. If GeneXpert results turn out negative a next step could be

ultrasound-guided core needle biopsy, which has been found to be frequently diagnostic when pathology services are available [(145, 146)].

Appendix: Focused assessment with Sonography for HIV-associated TB (FASH)

The above-mentioned characteristic findings of HIV associated extra-pulmonary TB consisting of pericardial, pleural and abdominal effusions, enlarged lymph nodes and focal splenic lesions are frequently seen in high prevalence settings. This observation led to the development of a short focused ultrasound protocol to help in settings with a shortage of skilled sonographers [(13, 147)]. Briefly, the method searches for effusions based on the approach used in the FAST protocol developed in emergency medicine [(148)]. Additionally, the examiner uses the same ultrasound windows to look for other findings suggestive of TB that are sufficiently easy to recognise and adequately specific to influence diagnostic reasoning [Figure 34].

Figure 34 FASH examination: probe position and possible findings in HIV associated TB.

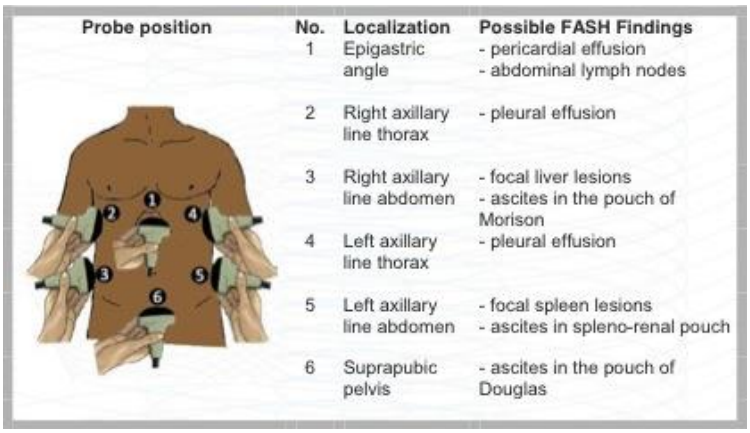

The 'FASH method' is widely used by emergency physicians in South Africa [(149)], other settings in Sub-Saharan Africa, as well as in areas of Asia where there is a high prevalence of TB and HIV like India and Indonesia [(14, 74, 77, 150)]. The use of the FASH protocol in paediatric patients has also been explored [(151)]. It was found that it is feasible and helpful, although in children the findings of disseminated TB seem to correlate more with a younger

age rather than with HIV status, possibly due to the immaturity of the immune response against mycobacterial infections in infants [(151, 152)].

It was shown early on that the protocol can be taught to clinicians with relatively little experience in imaging and sufficient diagnostic skills may be achieved in a few days [(153)]. Low-cost materials are available to teach the protocol [(154)]. With increasing availability of reasonably fast internet connections in sub-Saharan Africa and other low-resource settings, remotely supported and supervised approaches have become feasible [(155, 156)] and short training periods can be supported by subsequent remote expert advice [(157)]. Focused approaches like FASH may help to narrow the gap between the extensive number of patients in need of imaging and the scarce number of trained sonographers in many areas of the world. The FASH approach may serve as a model for the development of protocols for other diseases prevalent in areas with limited access to imaging, such as cystic echinococcosis in rural South America or schistosomiasis in West Africa [(158-160)].

References

1. Wallrauch C, Bärnighausen, T, Heller, T, Houlihan C, Newell M-L. The white and the three-letter plague: integration of TB and HIV care in sub-Saharan Africa. Future HIV Therapy 2008;2.
2. Selwyn PA, Hartel D, Lewis VA, Schoenbaum EE, Vermund SH, Klein RS, Walker AT, et al. A prospective study of the risk of tuberculosis among intravenous drug users with human immunodeficiency virus infection. N Engl J Med 1989;320:545-550.
3. Allen S, Batungwanayo J, Kerlikowske K, Lifson AR, Wolf W, Granich R, Taelman H, et al. Two-year incidence of tuberculosis in cohorts of HIV-infected and uninfected urban Rwandan women. Am Rev Respir Dis 1992;146:1439-1444.
4. Daley CL, Small PM, Schecter GF, Schoolnik GK, McAdam RA, Jacobs WR, Hopewell PC. An outbreak of tuberculosis with accelerated progression among persons infected with the human immunodeficiency virus. An analysis using restriction-fragment-length polymorphisms. N Engl J Med 1992;326:231-235.
5. Toossi Z, Johnson JL, Kanost RA, Wu M, Luzze H, Peters P, Okwera A, et al. Increased replication of HIV-1 at sites of Mycobacterium tuberculosis infection: potential mechanisms of viral activation. J Acquir Immune Defic Syndr 2001;28:1-8.
6. Collaborators GMaCoD. Global, regional, and national life expectancy, all-cause mortality, and cause-specific mortality for 249 causes of death, 1980-2015: a systematic analysis for the Global Burden of Disease Study 2015. Lancet 2016;388:1459-1544.
7. WHO. Consolidated guidelines on the use of antiretroviral drugs for treating and preventing HIV infection
Recommendations for a public health approach - Second edition. In; 2016.
8. WHO. Guidelines for managing advanced HIV disease and rapid initiation of antiretroviral therapy. In; 2017.

9. Moore RD, Chaisson RE. Natural history of opportunistic disease in an HIV-infected urban clinical cohort. Ann Intern Med 1996;124:633-642.
10. Kawooya MG, Muyinda Z, Byanyima R, E KM. Abdominal Ultrasound Findings in HIV Patients: a Pictorial Review. Ultrasound 2008;16:62-72.
11. Brunetti E, Brigada R, Poletti F, Maiocchi L, Garlaschelli AL, Gulizia R, Filice C. The current role of abdominal ultrasound in the clinical management of patients with AIDS. Ultraschall Med 2006;27:20-33.
12. Sidhu PS, Brabrand K, Cantisani V, Correas JM, Cui XW, D'Onofrio M, Essig M, et al. EFSUMB Guidelines on Interventional Ultrasound (INVUS), Part II. Diagnostic Ultrasound-Guided Interventional Procedures (Long Version). Ultraschall Med 2015;36:E15-35.
13. Dietrich CF, Goudie A, Chiorean L, Cui XW, Gilja OH, Dong Y, Abramowicz JS, et al. Point of Care Ultrasound: A WFUMB Position Paper. Ultrasound Med Biol 2017;43:49-58.
14. Heller T, Mtemang'ombe EA, Huson MA, Heuvelings CC, Bélard S, Janssen S, Phiri S, et al. Ultrasound for patients in a high HIV/tuberculosis prevalence setting: a needs assessment and review of focused applications for Sub-Saharan Africa. Int J Infect Dis 2017;56:229-236.
15. Tshibwabwa ET, Mwaba P, Bogle-Taylor J, Zumla A. Four-year study of abdominal ultrasound in 900 Central African adults with AIDS referred for diagnostic imaging. Abdom Imaging 2000;25:290-296.
16. Sienz M, Ignee A, Dietrich CF. [Reference values in abdominal ultrasound - liver and liver vessels]. Z.Gastroenterol. 2010;48:1141-1152.
17. Barreiros AP, Braden B, Schieferstein-Knauer C, Ignee A, Dietrich CF. Characteristics of intestinal tuberculosis in ultrasonographic techniques. Scand.J.Gastroenterol. 2008;43:1224-1231.
18. Trenker C, Gorg C, Jenssen C, Klein S, Neubauer A, Dietrich CF. [The role of abdominal ultrasound in hematological diseases]. Z Gastroenterol 2018;56:1063-1076.
19. Barreiros AP, Chiorean L, Braden B, Dietrich CF. Ultrasound in rare diffuse liver disease. Z Gastroenterol 2014;52:1247-1256.
20. Lindoso JA, Cota GF, da Cruz AM, Goto H, Maia-Elkhoury AN, Romero GA, de Sousa-Gomes ML, et al. Visceral leishmaniasis and HIV coinfection in Latin America. PLoS Negl Trop Dis 2014;8:e3136.
21. Dietrich CF, Lee JH, Herrmann G, Teuber G, Roth WK, Caspary WF, Zeuzem S. Enlargement of perihepatic lymph nodes in relation to liver histology and viremia in patients with chronic hepatitis C. Hepatology 1997;26:467-472.
22. Braden B, Faust D, Ignee A, Schreiber D, Hirche T, Dietrich CF. Clinical relevance of perihepatic lymphadenopathy in acute and chronic liver disease. J.Clin.Gastroenterol. 2008;42:931-936.
23. Schreiber-Dietrich D, Pohl M, Cui XW, Braden B, Dietrich CF, Chiorean L. Perihepatic lymphadenopathy in children with chronic viral hepatitis. J Ultrason 2015;15:137-150.
24. Dietrich CF, Leuschner MS, Zeuzem S, Herrmann G, Sarrazin C, Caspary WF, Leuschner UF. Peri-hepatic lymphadenopathy in primary biliary cirrhosis reflects progression of the disease. Eur.J.Gastroenterol.Hepatol. 1999;11:747-753.
25. Hirche TO, Russler J, Braden B, Schuessler G, Zeuzem S, Wehrmann T, Seifert H, et al. Sonographic detection of perihepatic lymphadenopathy is an indicator for primary sclerosing cholangitis in patients with inflammatory bowel disease. Int.J.Colorectal Dis. 2004;19:586-594.
26. Dong Y, Potthoff A, Klinger C, Barreiros AP, Pietrawski D, Dietrich CF. Ultrasound findings in autoimmune hepatitis. World J Gastroenterol 2018;24:1583-1590.

27. Ignee A, Jenssen C, Cui XW, Schuessler G, Dietrich CF. Intracavitary contrast-enhanced ultrasound in abscess drainage--feasibility and clinical value. Scand J Gastroenterol 2016;51:41-47.
28. Braden B, Helm B, Fabian T, Dietrich CF. [Bacillary angiomatosis of the liver, a suspected ultrasound diagnosis?]. Z Gastroenterol 2000;38:785-789.
29. Keane MA, Finlayson C, Joseph AE. A histological basis for the 'sonographic snowstorm' in opportunistic infection of the liver and spleen. Clin Radiol 1995;50:220-222.
30. Dietrich CF, Lorentzen T, Appelbaum L, Buscarini E, Cantisani V, Correas JM, Cui XW, et al. EFSUMB Guidelines on Interventional Ultrasound (INVUS), Part III - Abdominal Treatment Procedures (Long Version). Ultraschall Med 2016;37:E1-E32.
31. Reuss J, Seitz K, Rettenmaier G. Ultrasound diagnosis of hepatocellular carcinoma. Bildgebung 1993;60:18-22.
32. Society EAC. Guidelines, Version 9.1. In; 2018.
33. easloffice@easloffice.eu EAftSotLEa, Liver EAftSot. EASL Clinical Practice Guidelines: Management of hepatocellular carcinoma. J Hepatol 2018;69:182-236.
34. Merchante N, Figueruela B, Rodríguez-Fernández M, Rodríguez-Arrondo F, Revollo B, Ibarra S, Galindo MJ, et al. Low performance of ultrasound surveillance for the diagnosis of hepatocellular carcinoma in HIV-infected patients. AIDS 2019;33:269-278.
35. In.
36. Kim TK, Noh SY, Wilson SR, Kono Y, Piscaglia F, Jang HJ, Lyshchik A, et al. Contrast-enhanced ultrasound (CEUS) liver imaging reporting and data system (LI-RADS) 2017 - a review of important differences compared to the CT/MRI system. Clin Mol Hepatol 2017;23:280-289.
37. Piscaglia F, Wilson SR, Lyshchik A, Cosgrove D, Dietrich CF, Jang HJ, Kim TK, et al. American College of Radiology Contrast Enhanced Ultrasound Liver Imaging Reporting and Data System (CEUS LI-RADS) for the diagnosis of Hepatocellular Carcinoma: a pictorial essay. Ultraschall Med 2017;38:320-324.
38. Dietrich CF, Sharma M, Gibson RN, Schreiber-Dietrich D, Jenssen C. Fortuitously discovered liver lesions. World J Gastroenterol 2013;19:3173-3188.
39. Dietrich CF, Averkiou M, Nielsen MB, Barr RG, Burns PN, Calliada F, Cantisani V, et al. How to perform Contrast-Enhanced Ultrasound (CEUS). Ultrasound Int Open 2018;4:E2-E15.
40. Braden B, Faust D, Ignee A, Schreiber D, Hirche T, Dietrich CF. Clinical relevance of perihepatic lymphadenopathy in acute and chronic liver disease. J Clin Gastroenterol 2008;42:931-936.
41. Naseer M, Dailey FE, Juboori AA, Samiullah S, Tahan V. Epidemiology, determinants, and management of AIDS cholangiopathy: A review. World J Gastroenterol 2018;24:767-774.
42. Trenker C, Gorg C, Jenssen C, Klein S, Neubauer A, Wagner U, Dietrich CF. [Ultrasound in oncology, current perspectives]. Z Gastroenterol 2017;55:1021-1037.
43. Ignee A, Cui X, Hirche T, Demolo C, Barreiros AP, Schuessler G, Dietrich CF. Percutaneous biopsies of splenic lesions--a clinical and contrast enhanced ultrasound based algorithm. Clin Hemorheol Microcirc 2014;58:529-541.
44. von Herbay A, Barreiros AP, Ignee A, Westendorff J, Gregor M, Galle PR, Dietrich C. Contrast-enhanced ultrasonography with SonoVue: differentiation between benign and malignant lesions of the spleen. J Ultrasound Med 2009;28:421-434.
45. Cui XW, Ignee A, De Molo C, Schreiber-Dietrich D, Woenckhaus M, Dietrich CF. Littoral cell angioma of the spleen. Z Gastroenterol 2013;51:209-212.

46. Dong Y, Jurgensen C, Puri R, D'Onofrio M, Hocke M, Wang WP, Atkinson N, et al. Ultrasound imaging features of isolated pancreatic tuberculosis. Endosc Ultrasound 2018;7:119-127.
47. Dong Y, D'Onofrio M, Hocke M, Jenssen C, Potthoff A, Atkinson N, Ignee A, et al. Autoimmune pancreatitis: Imaging features. Endosc Ultrasound 2017.
48. Hirche TO, Ignee A, Barreiros AP, Schreiber-Dietrich D, Jungblut S, Ott M, Hirche H, et al. Indications and limitations of endoscopic ultrasound elastography for evaluation of focal pancreatic lesions. Endoscopy 2008;40:910-917.
49. Dietrich C. Transabdominal ultrasonography of the small and large intestine. In; 2018.
50. Bhaduri S, Wiselka MJ, Rogers PM. A review of ultrasound-guided percutaneous biopsy of the gastrointestinal tract in HIV-infected patients. HIV Med 1999;1:43-46.
51. Arora N, Gupta A, Sadeghi N. Primary effusion lymphoma: current concepts and management. Curr Opin Pulm Med 2017;23:365-370.
52. Auerbach E, Aboulafia DM. Venous and arterial thromboembolic complications associated with HIV infection and highly active antiretroviral therapy. Semin Thromb Hemost 2012;38:830-838.
53. Cui XW, Hocke M, Jenssen C, Ignee A, Klein S, Schreiber-Dietrich D, Dietrich CF. Conventional ultrasound for lymph node evaluation, update 2013. Z Gastroenterol 2014;52:212-221.
54. Hull MW, Phillips P, Montaner JSG. Changing global epidemiology of pulmonary manifestations of HIV/AIDS. Chest 2008;134:1287-1298.
55. Heuvelings CC, Bélard S, Janssen S, Wallrauch C, Grobusch MP, Brunetti E, Giordani MT, et al. Chest ultrasonography in patients with HIV: a case series and review of the literature. Infection 2016;44:1-10.
56. Giordani MT, Tamarozzi F, Kaminstein D, Brunetti E, Heller T. Point-of-care lung ultrasound for diagnosis of Pneumocystis jirovecii pneumonia: notes from the field. Crit Ultrasound J 2018;10:8.
57. Limonta S, Monge E, Montuori M, Morosi M, Galli M, Franzetti F. Lung ultrasound in the management of pneumocystis pneumonia: A case series. Int J STD AIDS 2018:956462418797872.
58. Ntsekhe M, Hakim J. Impact of human immunodeficiency virus infection on cardiovascular disease in Africa. Circulation 2005;112:3602-3607.
59. Longo-Mbenza B, Seghers KV, Phuati M, Bikangi FN, Mubagwa K. Heart involvement and HIV infection in African patients: determinants of survival. Int J Cardiol 1998;64:63-73.
60. Currie PF, Jacob AJ, Foreman AR, Elton RA, Brettle RP, Boon NA. Heart muscle disease related to HIV infection: prognostic implications. BMJ 1994;309:1605-1607.
61. Nzuobontane D, Blackett KN, Kuaban C. Cardiac involvement in HIV infected people in Yaounde, Cameroon. Postgrad Med J 2002;78:678-681.
62. Chiorean L, Cui XW, Klein SA, Budjan J, Sparchez Z, Radzina M, Jenssen C, et al. Clinical value of imaging for lymph nodes evaluation with particular emphasis on ultrasonography. Z Gastroenterol 2016;54:774-790.
63. Dietrich CF. Contrast-enhanced endobronchial ultrasound: Potential value of a new method. Endosc Ultrasound 2017;6:43-48.
64. Dietrich CF, Annema JT, Clementsen P, Cui XW, Borst MM, Jenssen C. Ultrasound techniques in the evaluation of the mediastinum, part I: endoscopic ultrasound (EUS), endobronchial ultrasound (EBUS) and transcutaneous mediastinal ultrasound (TMUS), introduction into ultrasound techniques. J Thorac Dis 2015;7:E311-325.

65. Sidhu PS, Cantisani V, Dietrich CF, Gilja OH, Saftoiu A, Bartels E, Bertolotto M, et al. The EFSUMB Guidelines and Recommendations for the Clinical Practice of Contrast-Enhanced Ultrasound (CEUS) in Non-Hepatic Applications: Update 2017 (Long Version). Ultraschall Med 2018;39:e2-e44.
66. Dietrich CF, Jenssen C, Herth FJ. Endobronchial ultrasound elastography. Endosc Ultrasound 2016;5:233-238.
67. Chiorean L, Barr RG, Braden B, Jenssen C, Cui XW, Hocke M, Schuler A, et al. Transcutaneous Ultrasound: Elastographic Lymph Node Evaluation. Current Clinical Applications and Literature Review. Ultrasound Med Biol 2016;42:16-30.
68. Mandel L. Ultrasound findings in HIV-positive patients with parotid gland swellings. J Oral Maxillofac Surg 2001;59:283-286.
69. Behr MA, Waters WR. Is tuberculosis a lymphatic disease with a pulmonary portal? Lancet Infect.Dis 2014;14:250-255.
70. Heller T, Goblirsch S, Bahlas S, Ahmed M, Giordani MT, Wallrauch C, Brunetti E. Diagnostic value of FASH ultrasound and chest X-ray in HIV-co-infected patients with abdominal tuberculosis. Int.J Tuberc.Lung Dis 2013;17:342-344.
71. Giordani MT, Brunetti E, Binazzi R, Benedetti P, Stecca C, Goblirsch S, Heller T. Extrapulmonary mycobacterial infections in a cohort of HIV-positive patients: ultrasound experience from Vicenza, Italy. Infection 2013;41:409-414.
72. Patel MN, Beningfield S, Burch V. Abdominal and pericardial ultrasound in suspected extrapulmonary or disseminated tuberculosis. S.Afr.Med J 2011;101:39-42.
73. Sinkala E, Gray S, Zulu I, Mudenda V, Zimba L, Vermund SH, Drobniewski F, et al. Clinical and ultrasonographic features of abdominal tuberculosis in HIV positive adults in Zambia. BMC.Infect.Dis 2009;9:44.
74. Mbanjumucyo G, Henwood PC. Focused assessment with sonography for HIV-associated tuberculosis (FASH) case series from a Rwandan district hospital. Afr J Emerg Med 2016;6:198-201.
75. Sculier D, Vannarith C, Pe R, Thai S, Kanara N, Borann S, Cain KP, et al. Performance of abdominal ultrasound for diagnosis of tuberculosis in HIV-infected persons living in Cambodia. J Acquir.Immune.Defic.Syndr. 2010;55:500-502.
76. Mandal A, Das SK, Bairagya TD. Presenting experience of managing abdominal tuberculosis at a tertiary care hospital in India. J Glob.Infect.Dis 2011;3:344-347.
77. Weber SF, Saravu K, Heller T, Kadavigere R, Vishwanath S, Gehring S, Bélard S, et al. Point-of-Care Ultrasound for Extrapulmonary Tuberculosis in India: A Prospective Cohort Study in HIV-Positive and HIV-Negative Presumptive Tuberculosis Patients. Am J Trop Med Hyg 2018;98:266-273.
78. Goblirsch S, Ahmed M, Brunetti E, Wallrauch C, Heller T. Ultrasound findings in cases of extrapulmonary TB in patients with HIV infection in Jeddah, Saudi Arabia. Asian Pac J Trop Dis 2014;4:14-17.
79. von Hahn T, Bange FC, Westhaus S, Rifai K, Attia D, Manns M, Potthoff A, et al. Ultrasound presentation of abdominal tuberculosis in a German tertiary care center. Scand.J Gastroenterol. 2014;49:184-190.
80. KORN RJ, KELLOW WF, HELLER P, CHOMET B, ZIMMERMAN HJ. Hepatic involvement in extrapulmonary tuberculosis; histologic and functional characteristics. Am J Med 1959;27:60-71.
81. Andrew WK, Thomas RG, Gollach BL. Miliary tuberculosis of the liver--another cause of the 'bright liver' on ultrasound examination. S Afr Med J 1982;62:808-809.

82. Kakkar C, Polnaya AM, Koteshwara P, Smiti S, Rajagopal KV, Arora A. Hepatic tuberculosis: a multimodality imaging review. Insights Imaging 2015;6:647-658.
83. Yu RS, Zhang SZ, Wu JJ, Li RF. Imaging diagnosis of 12 patients with hepatic tuberculosis. World J Gastroenterol 2004;10:1639-1642.
84. Cao BS, Li XL, Li N, Wang ZY. The nodular form of hepatic tuberculosis: contrast-enhanced ultrasonographic findings with pathologic correlation. J Ultrasound Med 2010;29:881-888.
85. Heller T, Goblirsch S, Wallrauch C, Lessells R, Brunetti E. Abdominal tuberculosis: sonographic diagnosis and treatment response in HIV-positive adults in rural South Africa. Int J Infect Dis 2010;14 Suppl 3:e108-112.
86. Koh DM, Burn PR, Mathews G, Nelson M, Healy JC. Abdominal computed tomographic findings of Mycobacterium tuberculosis and Mycobacterium avium intracellulare infection in HIV seropositive patients. Can Assoc Radiol J 2003;54:45-50.
87. dos Santos RP, Scheid KL, Willers DM, Goldani LZ. Comparative radiological features of disseminated disease due to Mycobacterium tuberculosis vs non-tuberculosis mycobacteria among AIDS patients in Brazil. BMC.Infect.Dis 2008;8:24.
88. Heller T, Bélard S, Wallrauch C, Carretto E, Lissandrin R, Filice C, Brunetti E. Patterns of Hepatosplenic Brucella Abscesses on Cross-Sectional Imaging: A Review of Clinical and Imaging Features. Am J Trop Med Hyg 2015;93:761-766.
89. Yu X, Yu J, Liang P, Liu F. Real-time contrast-enhanced ultrasound in diagnosing of focal spleen lesions. Eur J Radiol 2012;81:430-436.
90. Venkataramu NK, Gupta S, Sood BP, Gulati M, Rajawanshi A, Gupta SK, Suri S. Ultrasound guided fine needle aspiration biopsy of splenic lesions. Br J Radiol 1999;72:953-956.
91. Heller T, Wallrauch C, Brunetti E, Giordani MT. Changes of FASH ultrasound findings in TB-HIV patients during anti-tuberculosis treatment. Int J Tuberc Lung Dis 2014;18:837-839.
92. Atkinson NSS, Bryant RV, Dong Y, Maaser C, Kucharzik T, Maconi G, Asthana AK, et al. How to perform gastrointestinal ultrasound: Anatomy and normal findings. World J Gastroenterol 2017;23:6931-6941.
93. Atkinson NS, Bryant RV, Dong Y, Maaser C, Kucharzik T, Maconi G, Asthana AK, et al. WFUMB Position Paper. Learning Gastrointestinal Ultrasound: Theory and Practice. Ultrasound Med Biol 2016;42:2732-2742.
94. Dietrich CF, Lembcke B, Jenssen C, Hocke M, Ignee A, Hollerweger A. Intestinal ultrasound in rare gastrointestinal diseases, update, part 1. Ultraschall Med 2014;35:400-421.
95. Dietrich CF, Lembcke B, Jenssen C, Hocke M, Ignee A, Hollerweger A. Intestinal Ultrasound in Rare Gastrointestinal Diseases, Update, Part 2. Ultraschall Med 2015;36:428-456.
96. Yang G, Zhang W, Yu T, Meng J, Zhao D, Zhang X, Xu J, et al. The features of intestinal tuberculosis by contrast-enhanced ultrasound. Jpn J Radiol 2015;33:577-584.
97. Pereira JM, Madureira AJ, Vieira A, Ramos I. Abdominal tuberculosis: imaging features. Eur J Radiol 2005;55:173-180.
98. Ramaiya LI, Walter DF. Sonographic features of tuberculous peritonitis. Abdom Imaging 1993;18:23-26.
99. Bera C, Michael JS, Burad D, Shirly SB, Gibikote S, Ramakrishna B, Goel A, et al. Tissue Xpert™ MTB/Rif assay is of limited use in diagnosing peritoneal tuberculosis in patients with exudative ascites. Indian J Gastroenterol 2015;34:395-398.

100. Rufai SB, Singh S, Singh A, Kumar P, Singh J, Vishal A. Performance of Xpert MTB/RIF on Ascitic Fluid Samples for Detection of Abdominal Tuberculosis. J Lab Physicians 2017;9:47-52.
101. Wang J, Gao L, Tang S, Li T, Lei Y, Xie H, Liang J, et al. A retrospective analysis on the diagnostic value of ultrasound-guided percutaneous biopsy for peritoneal lesions. World J Surg Oncol 2013;11:251.
102. Qibi NM. New technique of blind peritoneal biopsy. Br Med J (Clin Res Ed) 1987;295:638.
103. Figueiredo AA, Lucon AM. Urogenital tuberculosis: update and review of 8961 cases from the world literature. Rev Urol 2008;10:207-217.
104. Ignee A, Straub B, Schuessler G, Dietrich CF. Contrast enhanced ultrasound of renal masses. World J Radiol 2010;2:15-31.
105. Vijayaraghavan SB, Kandasamy SV, Arul M, Prabhakar M, Dhinakaran CL, Palanisamy R. Spectrum of high-resolution sonographic features of urinary tuberculosis. J Ultrasound Med 2004;23:585-594.
106. Altez-Fernandez C, Ortiz V, Mirzazadeh M, Zegarra L, Seas C, Ugarte-Gil C. Diagnostic accuracy of nucleic acid amplification tests (NAATs) in urine for genitourinary tuberculosis: a systematic review and meta-analysis. BMC Infect Dis 2017;17:390.
107. Abbara A, Davidson RN, Medscape. Etiology and management of genitourinary tuberculosis. Nat Rev Urol 2011;8:678-688.
108. Matos MJ, Bacelar MT, Pinto P, Ramos I. Genitourinary tuberculosis. Eur J Radiol 2005;55:181-187.
109. Bilgin T, Karabay A, Dolar E, Develioğlu OH. Peritoneal tuberculosis with pelvic abdominal mass, ascites and elevated CA 125 mimicking advanced ovarian carcinoma: a series of 10 cases. Int J Gynecol Cancer 2001;11:290-294.
110. Huang WC, Tseng CW, Chang KM, Hsu JY, Chen JH, Shen GH. Usefulness of tumor marker CA-125 serum levels for the follow-up of therapeutic responses in tuberculosis patients with and without serositis. Jpn J Infect Dis 2011;64:367-372.
111. Lichtenstein D. Lung ultrasound in acute respiratory failure an introduction to the BLUE-protocol. Minerva Anestesiol 2009;75:313-317.
112. Hunter L, Bélard S, Janssen S, van Hoving DJ, Heller T. Miliary tuberculosis: sonographic pattern in chest ultrasound. Infection 2016;44:243-246.
113. Agostinis P, Copetti R, Lapini L, Badona Monteiro G, N'Deque A, Baritussio A. Chest ultrasound findings in pulmonary tuberculosis. Tropical Doctor. 2017;47:320-328.
114. Cao BS, Liang YM, Li XL, Deng J, Zhang GC. Contrast-enhanced sonography of juxtapleural pulmonary tuberculoma. J Ultrasound Med 2013;32:749-756.
115. Ferrer J. Pleural tuberculosis. Eur Respir J 1997;10:942-947.
116. Chen HJ, Hsu WH, Tu CY, Yu YH, Chiu KL, Hang LW, Hsia TC, et al. Sonographic septation in lymphocyte-rich exudative pleural effusions: a useful diagnostic predictor for tuberculosis. J Ultrasound Med 2006;25:857-863.
117. Lai YF, Su MC, Weng HH, Wu JT, Chiu CT. Sonographic septation: a predictor of sequelae of tuberculous pleurisy after treatment. Thorax 2009;64:806-809.
118. Denkinger CM, Schumacher SG, Boehme CC, Dendukuri N, Pai M, Steingart KR. Xpert MTB/RIF assay for the diagnosis of extrapulmonary tuberculosis: a systematic review and meta-analysis. Eur Respir J 2014;44:435-446.
119. Koegelenberg CF, Bolliger CT, Theron J, Walzl G, Wright CA, Louw M, Diacon AH. Direct comparison of the diagnostic yield of ultrasound-assisted Abrams and Tru-Cut needle biopsies for pleural tuberculosis. Thorax 2010;65:857-862.

120. Moseme T, Andronikou S. Through the eye of the suprasternal notch: point-of-care sonography for tuberculous mediastinal lymphadenopathy in children. Pediatr Radiol 2014;44:681-684.
121. Bosch-Marcet J, Serres-Créixams X, Zuasnabar-Cotro A, Codina-Puig X, Català-Puigbó M, Simon-Riazuelo JL. Comparison of ultrasound with plain radiography and CT for the detection of mediastinal lymphadenopathy in children with tuberculosis. Pediatr Radiol 2004;34:895-900.
122. Bosch-Marcet J, Serres-Créixams X, Borrás-Pérez V, Coll-Sibina MT, Guitet-Juliá M, Coll-Rosell E. Value of sonography for follow-up of mediastinal lymphadenopathy in children with tuberculosis. J Clin Ultrasound 2007;35:118-124.
123. Pool KL, Heuvelings CC, Bélard S, Grobusch MP, Zar HJ, Bulas D, Garra B, et al. Technical aspects of mediastinal ultrasound for pediatric pulmonary tuberculosis. Pediatr Radiol 2017;47:1839-1848.
124. Heuvelings CC, Bélard S, Andronikou S, Jamieson-Luff N, Grobusch MP, Zar HJ. Chest ultrasound findings in children with suspected pulmonary tuberculosis. Pediatr Pulmonol 2019.
125. Heller T, Lessells RJ, Wallrauch C, Brunetti E. Tuberculosis pericarditis with cardiac tamponade: management in the resource-limited setting. Am J Trop Med Hyg 2010;83:1311-1314.
126. Reuter H, Burgess LJ, Doubell AF. Epidemiology of pericardial effusions at a large academic hospital in South Africa. Epidemiol Infect 2005;133:393-399.
127. Mayosi BM, Burgess LJ, Doubell AF. Tuberculous pericarditis. Circulation 2005;112:3608-3616.
128. Desai HN. Tuberculous pericarditis. A review of 100 cases. S Afr Med J 1979;55:877-880.
129. Brindle HE, Allain TJ, Kampondeni S, Kayange N, Faragher B, Bates I, Joekes E. Utilization of ultrasound in medical inpatients in Malawi. Trans R Soc Trop Med Hyg 2013;107:405-410.
130. Pandie S, Peter JG, Kerbelker ZS, Meldau R, Theron G, Govender U, Ntsekhe M, et al. Diagnostic accuracy of quantitative PCR (Xpert MTB/RIF) for tuberculous pericarditis compared to adenosine deaminase and unstimulated interferon-γ in a high burden setting: a prospective study. BMC Med 2014;12:101.
131. Hakim JG, Ternouth I, Mushangi E, Siziya S, Robertson V, Malin A. Double blind randomised placebo controlled trial of adjunctive prednisolone in the treatment of effusive tuberculous pericarditis in HIV seropositive patients. Heart 2000;84:183-188.
132. Mayosi BM, Ntsekhe M, Bosch J, Pandie S, Jung H, Gumedze F, Pogue J, et al. Prednisolone and Mycobacterium indicus pranii in tuberculous pericarditis. N Engl J Med 2014;371:1121-1130.
133. Imazio M, Brucato A, Adler Y. A randomized trial of colchicine for acute pericarditis. N Engl J Med 2014;370:781.
134. Liebenberg JJ, Dold CJ, Olivier LR. A prospective investigation into the effect of colchicine on tuberculous pericarditis. Cardiovasc J Afr 2016;27:350-355.
135. Gopal S, Liomba NG, Montgomery ND, Moses A, Kaimila B, Nyasosela R, Chikasema M, et al. Characteristics and survival for HIV-associated multicentric Castleman disease in Malawi. J Int AIDS Soc 2015;18:20122.
136. Cui XW, Jenssen C, Saftoiu A, Ignee A, Dietrich CF. New ultrasound techniques for lymph node evaluation. World J Gastroenterol 2013;19:4850-4860.

137. Dietrich CF, Hocke M, Jenssen C. [Ultrasound for abdominal lymphadenopathy]. Dtsch Med Wochenschr 2013;138:1001-1018.
138. Ahuja AT, Ying M. Sonographic evaluation of cervical lymph nodes. AJR Am J Roentgenol 2005;184:1691-1699.
139. Tan R, Xiao Y, He Q. Ultrasound elastography: Its potential role in assessment of cervical lymphadenopathy. Acad Radiol 2010;17:849-855.
140. Bhatia KS, Cho CC, Yuen YH, Rasalkar DD, King AD, Ahuja AT. Real-time qualitative ultrasound elastography of cervical lymph nodes in routine clinical practice: interobserver agreement and correlation with malignancy. Ultrasound Med Biol 2010;36:1990-1997.
141. Jenssen C, Annema JT, Clementsen P, Cui XW, Borst MM, Dietrich CF. Ultrasound techniques in the evaluation of the mediastinum, part 2: mediastinal lymph node anatomy and diagnostic reach of ultrasound techniques, clinical work up of neoplastic and inflammatory mediastinal lymphadenopathy using ultrasound techniques and how to learn mediastinal endosonography. J Thorac Dis 2015;7:E439-458.
142. Cui XW, Ignee A, Bachmann Nielsen M, Schreiber-Dietrich D, Demolo C, Pirri C, Jedrejczyk M, et al. Contrast enhanced ultrasound of sentinel lymph nodes. Journal of Ultrasonography 2013;13:73-81.
143. Ligthelm LJ, Nicol MP, Hoek KG, Jacobson R, van Helden PD, Marais BJ, Warren RM, et al. Xpert MTB/RIF for rapid diagnosis of tuberculous lymphadenitis from fine-needle-aspiration biopsy specimens. J Clin Microbiol 2011;49:3967-3970.
144. Tadesse M, Abebe G, Abdissa K, Aragaw D, Abdella K, Bekele A, Bezabih M, et al. GeneXpert MTB/RIF Assay for the Diagnosis of Tuberculous Lymphadenitis on Concentrated Fine Needle Aspirates in High Tuberculosis Burden Settings. PLoS One 2015;10:e0137471.
145. Cheung YC, Wan YL, Lui KW, Lee KF. Sonographically guided core-needle biopsy in the diagnosis of superficial lymphadenopathy. J Clin Ultrasound 2000;28:283-289.
146. Wilson D, Nachega JB, Chaisson RE, Maartens G. Diagnostic yield of peripheral lymph node needle-core biopsies in HIV-infected adults with suspected smear-negative tuberculosis. Int J Tuberc Lung Dis 2005;9:220-222.
147. Heller T, Wallrauch C, Goblirsch S, Brunetti E. Focused assessment with sonography for HIV-associated tuberculosis (FASH): a short protocol and a pictorial review. Crit Ultrasound J 2012;4:21.
148. Scalea TM, Rodriguez A, Chiu WC, Brenneman FD, Fallon WF, Jr., Kato K, McKenney MG, et al. Focused Assessment with Sonography for Trauma (FAST): results from an international consensus conference. J Trauma 1999;46:466-472.
149. van Hoving DJ, Lamprecht HH, Stander M, Vallabh K, Fredericks D, Louw P, Muller M, et al. Adequacy of the emergency point-of-care ultrasound core curriculum for the local burden of disease in South Africa. Emerg Med J 2013;30:312-315.
150. Lee JB, Tse C, Keown T, Louthan M, Gabriel C, Anshus A, Hasjim B, et al. Evaluation of a point of care ultrasound curriculum for Indonesian physicians taught by first-year medical students. World J Emerg Med 2017;8:281-286.
151. Belard S, Heller T, Grobusch MP, Zar HJ. Point-of-care ultrasound: a simple protocol to improve diagnosis of childhood tuberculosis. Pediatric Radiology 2014;in press.
152. Bélard S, Heller T, Orie V, Heuvelings CC, Bateman L, Workman L, Grobusch MP, et al. Sonographic Findings of Abdominal Tuberculosis in Children With Pulmonary Tuberculosis. Pediatr Infect Dis J 2017;36:1224-1226.
153. Heller T, Wallrauch C, Lessells RJ, Goblirsch S, Brunetti E. Short course for focused assessment with sonography for human immunodeficiency virus/tuberculosis: preliminary

results in a rural setting in South Africa with high prevalence of human immunodeficiency virus and tuberculosis. Am.J Trop Med Hyg. 2010;82:512-515.
154. Heller T: FASH: Focused Assessment with Sonography for HIV/TB - A Practical Manual. In: TALC-Teaching Aids at Low Cost. Munich, Germany, 2013.
155. Janssen S, Grobusch MP, Heller T. 'Remote FASH' tele-sonography - a novel tool to assist diagnosing HIV-associated extrapulmonary tuberculosis in remote areas. Acta Trop 2013;127:53-55.
156. Janssen S, Basso F, Giordani MT, Brunetti E, Grobusch MP, Heller T. Sonographic findings in the diagnosis of HIV-associated tuberculosis: image quality and inter-observer agreement in FASH vs. remote-FASH ultrasound. J Telemed.Telecare. 2013;19:491-493.
157. Canan T, Hoffman R, Schooley AL, Boas ZP, Schwab KE, Kahn DJ, Shih RYW, et al. Training Course in Focused
Assessment with Sonography for HIV/TB in HIV Prevalent Medical Centers in
Malawi. Journal of Global Radiology 2018;4
158. Bélard S, Tamarozzi F, Bustinduy AL, Wallrauch C, Grobusch MP, Kuhn W, Brunetti E, et al. Point-of-Care Ultrasound Assessment of Tropical Infectious Diseases--A Review of Applications and Perspectives. Am J Trop Med Hyg 2016;94:8-21.
159. Del Carpio M, Mercapide CH, Salvitti JC, Uchiumi L, Sustercic J, Panomarenko H, Moguilensky J, et al. Early diagnosis, treatment and follow-up of cystic echinococcosis in remote rural areas in Patagonia: impact of ultrasound training of non-specialists. PLoS Negl Trop Dis 2012;6:e1444.
160. Bonnard P, Boutouaba S, Diakhate I, Seck M, Dompnier JP, Riveau G. Learning curve of vesico-urinary ultrasonography in Schistosoma haematobium infection with WHO practical guide: a "simple to learn" examination. Am J Trop Med Hyg 2011;85:1071-1074.